The Journal of Immunology

RESEARCH ARTICLE | APRIL 01 2022

IL-2 Signaling Couples the MAPK and mTORC1 Axes to Promote T Cell Proliferation and Differentiation in Teleosts FREE

Pengfei Mu; ... et. al

J Immunol (2022) 208 (7): 1616–1631.
https://doi.org/10.4049/jimmunol.2100764

IL-2 Signaling Couples the MAPK and mTORC1 Axes to Promote T Cell Proliferation and Differentiation in Teleosts

Pengfei Mu,*,† Jieying Huo,*,† Xiaofeng Li,* Wanru Li,* Xiaomeng Li,* Jingqun Ao,† and Xinhua Chen*,†,‡

IL-2 is a pleiotropic cytokine that is critical for T cell immunity. Although the IL-2–mediated regulation of T cell immunity in mammals is relatively well understood, it remains largely unknown whether and how IL-2 regulates T cell immunity in lower vertebrates. To address this knowledge gap, we investigated the role played by IL-2 in the regulation of T cell response, as well as the associated underlying mechanisms in a teleost fish, large yellow croaker (*Larimichthys crocea*). We found that large yellow croaker (*L. crocea*) IL-2 (*Lc*IL-2) significantly promoted T cell proliferation both in vivo and in vitro; significantly induced the differentiation of Th1, Th2, regulatory T, and cytotoxic T cells while inhibiting Th17 differentiation; and participated in the elimination of invading pathogenic bacteria. Mechanistically, the binding of *Lc*IL-2 to its heterotrimer receptor complex (*Lc*IL-15Rα/*Lc*IL-2Rβ/*Lc*γc) triggered the conserved JAK–STAT5 pathway, which in turn regulated the expression of genes involved in T cell expansion, differentiation, and biological function. The MAPK and mammalian target of rapamycin complex 1 (mTORC1) axes, which are involved in TCR-mediated signaling, were also required for *Lc*IL-2–mediated T cell response. Collectively, our results demonstrated that fish IL-2 plays a comprehensive regulatory role in T cell response and highlighted the complex and delicate network regulating T cell–driven immune response. We propose that T cell immunity is regulated by the interplay between TCR signaling and cytokine signaling, and that this basic strategy evolved before the emergence of the tetrapod lineage. Our findings provide valuable insights into the regulatory mechanisms underlying T cell response in teleosts. ***The Journal of Immunology*****, 2022, 208: 1616–1631.**

Adaptive immunity has evolved to provide a broader and more finely tuned repertoire of recognition for both self- and non–self-antigens (1). T cells are the principal cell players in the adaptive immune response. In mammals, T cells exclusively express coreceptors: CD4 is expressed by the Th cell lineage, and CD8 is expressed by the cytotoxic T cell lineage (2). After T cell activation by APCs, $CD4^+$ T cells differentiate into various Th cell subsets that produce cytokines involved in the regulation of immune responses, while $CD8^+$ T cells develop into effector cytotoxic T cells that help to clear infected or tumorous cells from the body (3, 4). Despite T cells being vitally important in mediating immune response and clearing pathogen infection or tumor cells, they have the dual characters for adaptive immunity. Dysregulation or abnormality of T cells immunity could cause organ-specific autoimmunity disease, allergy, and asthma (5). The activation, differentiation, and function of T cells is governed by various signals, for instance, Ag-stimulated TCR and costimulatory receptor signaling, cytokine-mediated signaling, and energy-controlled signaling (6–9). Thus, precise regulation of T cell development is required to effectively control various infections and avoid autoimmune diseases (10).

Via specific receptors, cytokines such as IL trigger a cascade of intracellular signals that regulate nearly every phase of T cell development, including maturation in the thymus, activation, proliferation, differentiation, effector T cell function, and the self-renewal of memory cells (11). In murine models, IL-7 signaling is considered critical for T cell development in the thymus (12), while Ag-activated $CD4^+$ T cell differentiation is governed predominantly by cytokines, including IL-12 (Th1 cell differentiation) and IL-4 (Th2 cell differentiation) (13). In addition, the cytokine IL-15 is indispensable for rapid division of memory $CD8^+$ T cells following pathogen re-exposure (14). Furthermore, effective T cell function depends on cytokines. For example, Th1 cells secrete IFN-γ to enhance cellular immunity, while Th2 cells secrete IL-4 to enhance humoral immunity. However, cytokine dysregulation or cytokine signal obstruction leads to immune deficiency (8). When IL-7 signaling is blocked because of IL-7R knockout, mice suffer from a severe lack of T cells (15), while in IL-15–deficient mice, the development of memory $CD8^+$ T cells is severely inhibited (16). Therefore, cytokines affect almost all aspects of T cell development and function.

IL-2, which is mainly produced by activated $CD4^+$ T cells, is one of the best-known cytokines involved in T cell activation and is

*Key Laboratory of Marine Biotechnology of Fujian Province, Institute of Oceanology, Fujian Agriculture and Forestry University, Fuzhou, China; †Key Laboratory of Marine Biogenetic Resources, Third Institute of Oceanography, Ministry of Natural Resources, Xiamen, China; and ‡Laboratory for Marine Biology and Biotechnology, Qingdao National Laboratory for Marine Science and Technology, Qingdao, China

ORCID: 0000-0003-2379-7596 (X.C.).

Received for publication August 4, 2021. Accepted for publication January 27, 2022.

This work was supported by grants from the National Key R&D Program of China (Grant 2018YFD0900503), the National Natural Science Foundation of China (Grants U1905204, 31772874, and 42076104), the China Agriculture Research System of MOF and MARA (Grant CARS-47), and the "Double first-class" scientific and technological innovation capacity and enhancement cultivation plan of Fujian Agriculture and Forestry University (Grant KSYLP001).

Address correspondence and reprint requests to Prof. Xinhua Chen or Prof. Jingqun Ao, Fujian Agriculture and Forestry University, No. 15 Shangxiadian Road, Fuzhou 350002, China (X.C.) or Third Institute of Oceanography, Ministry of Natural Resources, 184 Daxue Road, Xiamen 361005, China (J.A.). E-mail addresses: chenxinhua@tio.org.cn (X.C.) or ajingqun@tio.org.cn (J.A.).

The online version of this article contains supplemental material.

Abbreviations used in this article: γc, common γ-chain; Co-IP, coimmunoprecipitation; CsA, cyclosporine A; CST, Cell Signaling Technology; 4E-BP1, eIF4E-binding protein 1; *Lc*IL-2, large yellow croaker (*Larimichthys crocea*) IL-2; MCE, MedChemExpress; mTOR, mammalian target of rapamycin; mTORC1, mammalian target of rapamycin complex 1; PBL, peripheral blood leukocyte; PKL, primary head kidney leukocyte; PSL, primary spleen leukocyte; r*Lc*IL-2, recombinant *Larimichthys crocea* IL-2 protein; Treg, regulatory T; Zap70, ζ-associated protein of 70 kDa.

instrumental for the proliferation and differentiation of $CD4^+$ and $CD8^+$ T cells (17). IL-2 promotes the differentiation of activated $CD4^+$ T cells into Th1 and Th2 cells by inducing the expression of the cytokine receptors IL-12Rβ and IL-4Rα, respectively (18–20). The duration and strength of the IL-2 signal affect the differentiation of effector cytotoxic T cells, as well as the generation of memory $CD8^+$ T cells (21, 22). Indeed, in both the primary and the secondary immune responses, $CD8^+$ T cell proliferation is severely inhibited in the absence of IL-2 (23). IL-2 also regulates the development and proliferation of regulatory T (Treg) cells, which are essential for maintenance of immune homeostasis (24, 25). IL-2 acts on various cell populations by binding to the high-affinity IL-2R, which consists of three components: IL-2Rα, IL-2Rβ, and common γ-chain (γc) (26, 27). Kinetically, IL-2 first binds to IL-2Rα, resulting in a conformational change in IL-2, followed by the recruitment of IL-2Rβ, and finally the recruitment of γC (28). The formation of the IL-2/IL-2R signaling complex triggers the JAK–STAT5 pathway, as well as the MAPK/Erk and mammalian target of rapamycin complex 1 (mTORC1) pathways, to synergistically regulate the expression of genes essential for T cell differentiation and function (28).

Fish are lower vertebrates, and fish ancestors possessed primordial T cells as early as ∼450 million years ago. Characterization of the initiation and regulation of T cell immunity in fish may thus help to clarify the evolution of adaptive immune systems. Recent studies have characterized several T cell populations, including $CD4^+$ and $CD8^+$ T cells, in fish; Th1-like–, Th2-like–, and Treg-mediated immune responses have also been investigated in several fish species (29–37). Moreover, the regulatory mechanisms underlying T cell immunity have been preliminarily demonstrated from a variety of perspectives in teleosts. These studies have demonstrated that MAPK/Erk cascade-mediated glycolysis, Ca^{2+}-calcineurin axis-controlled NFAT nuclear translocation, and NF-κB–induced IL-17 expression, in conjunction with mTORC1-coupled metabolic programming, collectively promote T cell immunity (38–41). However, these previous studies have mainly focused on TCR and costimulatory receptor-mediated events or on metabolism-controlled signaling. Thus, whether and how cytokine signaling modulates T cell immunity in lower vertebrates remains largely unknown. In a previous study, we identified and characterized an IL-2 gene from a teleost, the large yellow croaker (*Larimichthys crocea*) IL-2 (*Lc*IL-2); our results suggested that *Lc*IL-2 might be involved in the T cell response in this species (42). In this study, we further study both the precise functions of *Lc*IL-2 in T cell response and the mechanisms underlying these functions. We demonstrated that *Lc*IL-2 promotes T cell proliferation and differentiation, as well as ensures the clearance of pathogenic bacteria. We found that *Lc*IL-2 initiates JAK–STAT5 signaling through its receptor complex *Lc*IL-15Rα/*Lc*IL-2Rβ/*Lc*γc to regulate T cell immunity. More importantly, MAPK and mTORC1 axes activated by *Lc*IL-2 strengthen this process. Thus, this study comprehensively revealed the signal pathways by which IL-2 regulates T cell response in a teleost. Our data suggest that modulation of T cell response by IL-2 may be an ancestral strategy that predated the divergence of tetrapods from teleosts, thus providing valuable insight into the evolution of adaptive immunity.

Materials and Methods

Experimental fish

Large yellow croakers (101.6 ± 21.9 g) were purchased from a mariculture farm in Ningde, Fujian, China. Fish were raised at 20 ± 2°C with a flow-through seawater supply and were fed commercial feed pellets twice a day. After a 7-d acclimation period, healthy fish were used for the following experiments. This study was performed in strict accordance with the Regulations of the Administration of Affairs Concerning Experimental Animals established by the Fujian Provincial Department of Science and Technology. All surgeries were performed under Tricaine-S anesthesia, and all efforts were made to minimize suffering.

Sequence analysis

The cDNA and amino acid sequences of IL-15Rα, IL-2Rβ, γC, JAK1/3, STAT5a/b, Mek1/2, Erk1/2, and mTOR of large yellow croaker were obtained from whole-genome sequence with the accession number JRPU02000000 and the project PRJNA245366 in National Center for Biotechnology Information (NCBI) GenBank (https://www.ncbi.nlm.nih.gov/nuccore/JRPU00000000.2/) (43). The sequences of human IL-2Rα, IL-2Rβ, γC, JAK1/3, STAT5a/b, Mek1/2, Erk1/2, and mTOR were obtained from the National Center for Biotechnology Information GenBank (https://www.ncbi.nlm.nih.gov/). Potential functional domains of IL-2Rα/IL-15Rα, IL-2Rβ, γC, JAK1/3, STAT5a/b, Mek1/2, Erk1/2, and mTOR were predicted using SMART version 4.0 (https://smart.embl.de/), and domain organization was visualized using DOG version 2.0. The tertiary structures of the IL-2Rα/IL-15Rα, IL-2Rβ, γC, JAK1/3, STAT5a/b, Mek1/2, Erk1/2, and mTOR proteins were predicted using SWISS-MODEL on the ExPASy server (https://swissmodel.expasy.org/interactive) and visualized using PyMOL. The accession numbers of the molecules included in this study are listed in Supplemental Table I.

Preparation of primary immune-related cells

Large yellow croaker primary peripheral blood leukocytes (PBLs), primary head kidney leukocytes (PKLs), and primary spleen leukocytes (PSLs) were prepared as described previously (44). Briefly, blood was drawn from the caudal vein of a large yellow croaker and immediately diluted 10 times with DMEM containing 15 IU/ml heparin sodium. Then, the head kidney and spleen were removed from the freshly killed fish under sterile conditions. Each organ was gently pushed through a 70-μm nylon mesh (BD) to yield single-cell suspensions. The cell suspensions were washed twice with ice-cold DMEM containing 2% FBS (Life Technologies), 15 IU/ml heparin, and 2% penicillin/streptomycin (Life Technologies). Each diluted blood sample or single-cell suspension was loaded onto a freshly prepared 34%/51% Percoll (GE) density gradient and separated via centrifugation at 650 × *g* for 30 min at 4°C. The PBLs, PKLs, or PSLs at the gradient interface were collected and washed twice with DMEM. The washed PBLs, PKLs, or PSLs were resuspended in DMEM containing 2% FBS and 1% penicillin/streptomycin. The prepared suspensions were used in subsequent experiments.

In vivo T cell proliferation assays

Large yellow croakers were i.p. injected with 20 μg of purified recombinant *L. crocea* IL-2 protein (r*Lc*IL-2) per 100 g body weight (n = 15 fish). Fish were injected with BSA at the same dosage as controls. At 40 h after injection, both groups of fish were further injected with 250 μg of EdU (Invitrogen) dissolved in 100 μl PBS per 100 g body weight. After a further 8 h, all fish were killed. The PBLs, PKLs, and PSLs (2×10^6 cells each) were immediately prepared as described earlier. Isolated PBLs, PKLs, or PSLs (2×10^6 cells) were incubated with FITC-conjugated mouse anti-large yellow croaker IgM mAb (prepared by our laboratory) at 4°C for 30 min to detect IgM^+ B cells (45) and then washed three times with PBS (pH 7.4) containing 2% BSA. Then cells were fixed with Fixation/Permeabilization Solution (BD) for 20 min at room temperature and then washed three times with 1×Permeabilization Buffer (Invitrogen). The fixed cells were incubated with Alexa Fluor 647–conjugated rabbit anti–ζ-associated protein of 70 kDa (anti-Zap70) mAbs (2707; Cell Signaling Technology [CST]) for 30 min at 4°C for T cell detection. After washing three times with 1×Permeabilization Buffer, the EdU^+ cells were detected by click reaction using a Click-iT EdU Pacific Blue Flow Cytometry Assay Kit (Invitrogen), following the manufacturer's instructions. Finally, cells were analyzed with a flow cytometer (FACSymphony A3; BD) and FlowJo software (Tree Star).

In vitro T cell proliferation assays

To determine the effects of *Lc*IL-2 on T cell proliferation in vitro, we labeled 5×10^6 PKLs using CellTrace Violet (Thermo Fisher), following the manufacturer's instructions. In brief, cells were incubated with 5 μM CellTrace Violet for 10 min at room temperature and washed twice with DMEM. The labeled cells were cultured in DMEM (10% FBS) containing 200 ng/ml r*Lc*IL-2 in the presence or absence of 1 μg/ml PHA at 28°C. Cells were sampled after 3 and 6 d of culture. LIVE/DEAD Fixable Near-IR Dead Cell Stain (L34975; Thermo Fisher) was added to each cell suspension to determine cell viability prior to fixation and permeabilization. The T cells were then labeled with anti-Zap70 mAbs as described earlier, and the fluorescence intensity of CellTrace Violet in the viable T cells was analyzed using a flow cytometer (FACSymphony A3; BD) as a measure of cell division.

Gene expression analysis by real-time quantitative PCR

To further determine the effects of *Lc*IL-2 on T cell proliferation and differentiation in vitro, we stimulated 5×10^6 PKLs with r*Lc*IL-2 (200 ng/ml) or BSA (200 ng/ml) in the presence or absence of 1 μg/ml PHA for 24 h at 28°C. The cultured cells were sampled for total RNA extraction using the Eastep Super Total RNA Extraction Kit (Promega). The cDNA was synthesized using GoScript Reverse Transcription Mix (Promega) with oligo(dT) primers. The cDNA samples were diluted 20 times in nuclease-free water for real-time PCRs. The real-time PCRs analysis was performed using TB Green mix (Takara) and specific primers (Supplemental Table II) on a QuantStudio5 instrument (Thermo Fisher). All reactions were run in triplicate on 96-well plates. Gene expression levels were normalized against the reference gene *Lc*β-actin using the $2^{-\Delta\Delta CT}$ method (46, 47). The fold change in gene expression level at each time point was calculated by comparing the normalized gene expression level in the r*Lc*IL-2–stimulated group with that in the BSA-stimulated group. All data were obtained from three independent experiments, and each analysis was performed in triplicate.

Western blots

To specifically detect the protein expression patterns of Zap70 after r*Lc*IL-2 induction, we performed Western blots. A total of 2×10^7 PBLs, PKLs, or PSLs were lysed in radioimmunoprecipitation assay buffer (P0013B; Beyotime). After centrifugation at 13,000 × *g* for 30 min, the supernatants of the cell lysates were separated using PAGE and electrophoretically transferred onto polyvinylidene fluoride membranes (GE). After blocking with 5% skim milk in TBST buffer (25 mM Tris–HCl, 137 mM NaCl, 2.7 mM KCl, and 0.05% Tween 20 [pH 7.4]), the membranes were incubated with 1:2000 diluted rabbit anti-Zap70 mAb (2707; CST) at 4°C overnight. After incubation, the membranes were washed three times with TBST buffer before a second incubation with 1:5000 diluted goat anti-rabbit IgG Ab conjugated with HRP (AP307P; Sigma) at room temperature for 1 h. Rabbit anti–β-actin Ab (1:5000) (AF7018; Affinity) was used as the primary Ab to ensure equal loading.

Cyclosporine A treatment

To inhibit *Lc*IL-2 expression in vitro, we stimulated 2×10^6 PKLs with 10 μg/ml PHA in the presence or absence of 2 nM cyclosporine A (CsA; HY-B0579, MedChemExpress [MCE]) for 24 h. Cells were then collected, and *Lc*IL-2 expression was measured using real-time PCR. To analyze the T cell proliferation when *Lc*IL-2 expression was inhibited by CsA in vivo, we i.p. injected normal large yellow croakers (n = 6 fish per treatment) with 100 μl CsA at a dosage of 1.5 mg per 100 g body weight for 2 consecutive days. The same volume of PBS was injected as a control. Forty hours later, both groups of fish were injected with 250 μg EdU dissolved in 100 μl PBS per 100 g body weight. At 8 h postinjection, all fish were killed. The PBLs, PKLs, and PSLs were isolated for detection of the EdU incorporation in T cell as described earlier.

Bacterial challenge

To further analyze the function of *Lc*IL-2 in bacterial clearance in large yellow croaker, we i.p. injected 150 fish with 200 μl of 1×10^4 CFUs/ml *Pseudomonas plecoglossicida*, an important pathogen (48), per 100 g body weight; 50 blank control fish were injected with 200 μL PBS only. The infected fish were randomly divided among three treatment groups (n = 50 per group) and injected with 10 μg r*Lc*IL-2 per 100 g body weight, 1.5 mg CsA per 100 g body weight, or 200 μl PBS. Fish were identically reinjected every 2 d for 6 d. Cumulative survival was monitored for 7 d after the bacterial challenge. The cumulative survival data from the challenge experiments were analyzed using Kaplan–Meier methods, and differences among groups were assessed using log-rank tests. The blood, head kidneys, and spleens of six surviving fish in each group at 7 d postinfection were collected for T cell proliferation as described earlier. The head kidneys and spleens of another three fish in each group were collected for total RNA and genomic DNA extraction. Total RNA was used to synthesize cDNA, and real-time PCRs were performed to detect the expression of genes associated with effective T cell function (IFN-γ, Granzyme B, Perfron A, LT-α, and FasL). We specifically amplified the *P. plecoglossicida* genes *rpoD* and *gyrB* using real-time PCR with fish genomic DNA as the template. Relative *P. plecoglossicida* abundance was normalized against the reference gene *Lc*β-actin using the $2^{-\Delta\Delta CT}$ method (47). GenBank accession numbers and primer sequences for *rpoD* and *gyrB* are given in Supplemental Table II.

Plasmid construction and coimmunoprecipitation assays

We constructed 11 plasmids by subcloning the following gene fragments: the LcIL-2 open reading frame deleting the fragment encoding signal peptide (L^{20}-A^{141}, pCMV-Flag-IL-2), the *Lc*IL-15Rα gene fragment encoding the extracellular region (G^{24}-S^{184}, pcDNA-V5-IL-15Rα-E), the *Lc*IL-2Rβ gene fragment encoding the extracellular region (H^{21}-T^{241}) and the intracellular region (C^{264}-I^{551}) (pCMV-HA-IL-2Rβ-E, pCMV-HA-IL-2Rβ-In), the *Lc*γc gene fragments encoding the extracellular (K^{18}-M^{218}) and the intracellular (H^{242}-V^{347}) regions (pcDNA3.1-myc-γc-E, pcDNA3.1-myc-γc-In, pCMV-Flag-γc-In), the JAK1 gene fragment encoding the FERM and SH2 domains (M^1-R^{542}, pCMV-Flag-JAK1), the JAK3 gene fragment encoding the FERM and SH2 domains (M^1-G^{500}, pcDNA3.1-myc-JAK3), the full-length open reading frame of STAT5a (M^1-S^{786}, pcDNA-V5-STAT5a), and the full-length open reading frame of STAT5b (M^1-G^{784}, pcDNA-V5-STAT5b). The primers used to amplify the gene fragments are listed in Supplemental Table II.

For the coimmunoprecipitation (Co-IP) assays, HEK-293T cells were seeded into 10-cm cell culture dishes (4×10^6 cells/dish), incubated overnight, and then transfected with the indicated expression plasmids using FuGENE HD transfection reagent (E2311; Promega). At 36 h posttransfection, the cells were washed with ice-cold PBS and lysed with 400 μl IP cell lysis buffer (P0013; Beyotime). After centrifugation at 13,000 × *g* for 30 min at 4°C, the supernatants of the cell lysates were immunoprecipitated using anti-Flag M2 Affinity Gel (A2220; Sigma), anti–V5-tag mAb-Magnetic Agarose (M167-10; MBL), or anti–myc-tag mAb-Magnetic Agarose (M047-10; MBL). The precipitates were washed 10 times with lysis buer and then eluted by boiling the pellets with 5× SDS-PAGE loading buer. Finally, the eluted samples were Western blotted with rabbit anti-Flag mAb (ab205606; Abcam), rabbit anti-V5 mAb (ab206566; Abcam), rabbit anti-HA mAb (H6908; Sigma), or rabbit anti-myc mAb (C3956; Sigma).

Phosphorylation analysis

Isolated 2×10^7 PKLs were incubated with r*Lc*IL-2 at a final concentration of 200 ng/ml for 10, 30, or 45 min at 28°C. The equal number of PKLs without any treatment were used as the resting control. The treated and resting cells were harvested and lysed in radioimmunoprecipitation assay buffer for Western blots. Western blots were performed as described earlier with the following Abs: rabbit anti-STAT5a/b (ab194898; Abcam), rabbit anti-pSTAT5 Tyr694 (ab32364; Abcam), rabbit anti-Mek1/2 (8727; CST), rabbit anti-pMek1/2 Ser217/218 (9154; CST), rabbit anti-Erk1/2 (4695; CST), rabbit anti-pErk1/2 Thr202/Tyr204 (9101; CST), rabbit anti-mTOR (2983; CST), rabbit anti-pmTOR Ser-2481 (MA5-33139; Thermo Fisher), rabbit anti–eIF4E-binding protein 1 (anti–4E-BP1; 9644; CST), or rabbit anti-p4E-BP1 Thr37/46 (2855; CST). Phosphorylated AKT was detected using a phos-tag SDS-PAGE gel (Wako), following the manufacturer's instructions. The cell lysates were separated using 8% Phos-tag SDS-PAGE gels and blotted onto polyvinylidene fluoride membranes for Western blot analysis with rabbit anti-AKT (AF6261; Affinity) as the primary Ab.

Immunofluorescence microscopy

Isolated 5×10^5 PKLs were seeded onto poly-L-lysine–treated slides in 24-well plates and cultured for 3 h. Cultured cells were stimulated with r*Lc*IL-2 at a final concentration of 200 ng/ml for 30 min and then fixed in Fixation/Permeabilization Solution for 20 min at room temperature. The fixed cells were blocked with 5% normal goat serum and incubated with rabbit anti-pSTAT5 Tyr694, rabbit anti-pMek1/2 Ser217/218, rabbit anti-pErk1/2 Thr202/Tyr204, rabbit anti-pmTOR Ser-2481, or rabbit anti-p4E-BP1 Thr37/46 Ab as described earlier overnight at 4°C. After incubation, cells were reincubated with Alexa Fluor 488–conjugated goat anti-mouse IgG (Abcam) and Alexa Fluor 647–conjugated goat anti-rabbit IgG (Abcam) for 1 h at 37°C. Each incubation was carried out in an immunohistochemical wet box and terminated by washing the cells three times with PBST. Finally, the slides were mounted with an antifade solution containing DAPI and observed under a laser scanning confocal microscope (Leica). The immunofluorescence intensity was analyzed by Leica software.

Specific inhibitor treatment

To inhibit the STAT5-dependent JAK–STAT pathway, MAPK pathway, and mTORC1 axis in vitro, we treated isolated PKLs with STAT5 inhibitor STAT5-IN-1 (HY-101853; MCE) at a final concentration of 50 μM, Erk inhibitor SCH772984 (HY-50846; MCE) at a final concentration of 20 nM, or mTORC1 inhibitor rapamycin (HY-10219; MCE) at a final concentration of 10 nM for 3 h, respectively. Then, r*Lc*IL-2 was added to all cells at a final concentration of 200 ng/ml. The stimulated cells were collected at indicated time points for Western blots or at 24 h for real-time PCR. To determine the effect of *Lc*IL-2 on T cell proliferation when JAK–STAT5, MAPK/Erk, or

mTORC1 signaling was blocked by a specific inhibitor in vitro, we labeled isolated PKLs with CellTrace Violet as described earlier. The labeled cells were treated with specific inhibitor STAT5-IN-1 (50 μM), SCH772984 (20 nM), or rapamycin (10 nM) for 3 h before stimulation with PHA (1 μg/ml) and r*Lc*IL-2 (200 ng/ml). After culture for 6 d, the treated cells were collected for detecting the T cell proliferation as described earlier.

Preparation of polyclonal Abs

Gene fragments from the receptor subunits *Lc*IL-15Rα and *Lc*IL-2Rβ that encode the extracellular regions (*Lc*IL-15Rα$^{24–188\ aa}$ and *Lc*IL-2Rβ$^{21–240\ aa}$, respectively) were amplified with specific primers (Supplemental Table II) and subcloned into separate pET-28a vectors. Recombinant *Lc*IL-15Rα and *Lc*IL-2Rβ extracellular regions (r*Lc*IL-15Rα and r*Lc*IL-2Rβ, respectively) were induced with 0.5 mM isopropyl-β-D-thiogalactopyranoside and purified under denaturing condition using the Ni Sepharose 6 Fast Flow Purification System (GE Healthcare Life Sciences). Purified r*Lc*IL-15Rα and r*Lc*IL-2Rβ were quantified with a NanoDrop 1000 spectrometer (Thermo Fisher) and used for the preparation of polyclonal Abs.

Six-week-old male BALB/c mice were immunized with 20 μg purified r*Lc*IL-15Rα in CFA, and 6-wk-old male New Zealand white rabbits were immunized with 100 μg purified r*Lc*IL-2Rβ in CFA. Both mice and rabbits were immunized four times at biweekly intervals. A week after the final immunization, blood samples were taken from the mice and rabbits, and Ab titers in the sera were measured using ELISA with the corresponding recombinant proteins adsorbed to the solid phase. When the Ab titers were >1:10,000, mice and rabbits were bled. Mouse anti–*Lc*IL-15Rα and rabbit anti–*Lc*IL-2Rβ polyclonal Abs were preadsorbed using *Escherichia coli* lysate supernatants to remove the irrelevant Abs and then purified using HiTrap Protein A HP column on an AKTA prime Plus instrument following the manufacturer's instructions (GE Healthcare). Nonspecific mouse and rabbit Abs were purified from unimmunized mice and rabbits as controls, respectively. The obtained polyclonal Abs were stored at −80°C until use.

LcIL-15Rα– and/or LcIL-2Rβ–blocking assays

To explore whether *Lc*IL-15Rα and *Lc*IL-2Rβ participate in *Lc*IL-2–induced signal transduction, we performed *Lc*IL-15Rα- and/or *Lc*IL-2Rβ-blocking assays using mouse anti–*Lc*IL-15Rα and rabbit anti–*Lc*IL-2Rβ polyclonal Abs. PKLs (2×10^7 cells/ml) were cultured in 10 ml DMEM containing 10% FBS and 1% penicillin/streptomycin for 3 h. Then, PKLs were treated with mouse anti–*Lc*IL-15Rα Ab (2 μg/ml) and/or rabbit anti–*Lc*IL-2Rβ Ab (2 μg/ml) for 30 min, followed by stimulation with r*Lc*IL-2 (200 ng/ml). The stimulated cells were collected at 30 min for Western blots or at 24 h for real-time PCR. To determine the effect of *Lc*IL-2 on T cell proliferation when *Lc*IL-15Rα and/or *Lc*IL-2Rβ was blocked by corresponding Ab, we labeled isolated PKLs with CellTrace Violet. The labeled cells were treated with mouse anti–*Lc*IL-15Rα Ab (2 μg/ml) and/or rabbit anti–*Lc*IL-2Rβ Ab (2 μg/ml) for 30 min, followed by stimulation with PHA (1 μg/ml) and r*Lc*IL-2 (200 ng/ml). After culture for 6 d, the treated cells were collected for detecting the T cell proliferation as described earlier.

Statistical analyses

All statistical analyses were performed using SPSS 20.0 (SPSS Inc.). All data are expressed as mean ± SD. The cumulative survival data from the challenge experiments were analyzed using Kaplan–Meier methods, and differences among groups were assessed using log-rank tests. For all other data, significant differences among means were identified using unpaired Student *t* tests.

Results

IL-2 plays a pivotal role in T cell proliferation in large yellow croaker

IL-2 acts as a T cell growth factor in mammals (49). To test whether IL-2 participates in T cell proliferation in the large yellow croaker, we first measured the in vivo proliferation of Zap70$^+$ T cells stained with EdU. The EdU content of the Zap70$^+$ T cells from the PBLs, PKLs, and PSLs was monitored using flow cytometry (Fig. 1A). Significantly more EdU$^+$ Zap70$^+$ T cells were found in the PBLs, PKLs, and PSLs from the r*Lc*IL-2–injected fish as compared with the BSA-injected control fish (Fig. 1B–1E). In addition, the mRNA expression levels of the T cell marker genes CD3ζ, CD4-1, CD8α, and Zap70 were significantly upregulated in the PBLs, PKLs, and PSLs from the r*Lc*IL-2–stimulated fish as compared with those from the BSA-injected control fish (Fig. 1F). Finally, Zap70 protein expression was also noticeably greater in the PBLs, PKLs, and PSLs from the r*Lc*IL-2–stimulated fish as compared with the BSA-injected control fish (Fig. 1G). Thus, our results indicated that *Lc*IL-2 promoted T cell proliferation in vivo.

To verify that *Lc*IL-2 increased T cell proliferation in vitro, we stimulated CellTrace Violet–labeled lymphocytes with r*Lc*IL-2 in the presence or absence of PHA. The effects of *Lc*IL-2 on the proliferation of T cells were monitored by flow cytometry (Fig. 1H). When lymphocytes were stimulated with r*Lc*IL-2 alone, T cell proliferation was observed only at 6 d poststimulation (Fig. 1I, 1J). In the presence of PHA, r*Lc*IL-2 significantly increased T cell proliferation at both 3 and 6 d poststimulation (Fig. 1I, 1K). T cell marker genes (CD3ζ, CD4-1, CD8α, and Zap70) were also significantly upregulated at 6 d after r*Lc*IL-2 stimulation, irrespective of PHA (Fig. 1L). Thus, our results indicated that *Lc*IL-2 induced the proliferation of T cells, particularly activated T cells, in vitro.

IL-2 is involved in T cell differentiation

Given that *Lc*IL-2 induced T cell proliferation, we next investigated the effects of *Lc*IL-2 on T cell differentiation. Because we lack appropriate Abs with which to distinguish T cell subsets in the large yellow croaker, gene expression levels were used to reflect T cell differentiation. The Th1-associated genes IFN-γ and T-bet were significantly upregulated in response to r*Lc*IL-2 stimulation (Fig. 2A), as were the Th2-associated genes IL-4/13A, IL-4/13B, and GATA-3 (Fig. 2B) and the Treg-associated genes Foxp3 and CTLA-4 (Fig. 2C). By contrast, the Th17 cytokine genes IL-17A/F2 and IL17A/F3 and transcription factor gene RORγ were significantly downregulated in response to r*Lc*IL-2 (Fig. 2D). However, four genes associated with the cytotoxic activity of CD8$^+$ T cells (perforin A, granzyme B, LT-α, and FasL) were significantly upregulated in response to r*Lc*IL-2 (Fig. 2E). These results indicated that *Lc*IL-2 played a role in the regulation of CD4$^+$ and CD8$^+$ T cell development and differentiation.

IL-2 facilitates T cell–mediated infection elimination in the large yellow croaker

CsA is an immunosuppressive drug that effectively inhibits IL-2 production in mammals (17, 50). Previously, we showed that *Lc*IL-2 transcription was dramatically increased in PKLs in response to PHA (42). To test whether CsA suppressed *Lc*IL-2 expression in the large yellow croaker, we treated PKLs with PHA in the presence and absence of CsA. PHA alone markedly increased the mRNA expression of *Lc*IL-2 in PKLs, but this PHA-induced upregulation of *Lc*IL-2 was severely inhibited in the presence of CsA (Fig. 3A), suggesting that CsA may suppress *Lc*IL-2 expression in the large yellow croaker. Subsequent in vivo experiments confirmed that *Lc*IL-2, as well as the T cell–associated genes CD3ζ, CD4-1, and CD8α, were significantly downregulated in the PBLs, PKLs, and PSLs from the CsA-treated large yellow croakers as compared with the PBS-treated controls (Fig. 3B, 3C). T cell proliferation was also significantly decreased in the PBLs, PKLs, and PSLs from the CsA-treated fish as compared with the controls (Fig. 3D–H). These results suggested that CsA effectively suppressed *Lc*IL-2 production and the *Lc*IL-2–mediated T cell response in large yellow croakers.

To test the efficacy of the *Lc*IL-2–mediated T cell response in the presence of CsA, we performed infection experiments with *P. plecoglossicida*. We found that administration of r*Lc*IL-2 significantly promoted the proliferation of T cells (Fig. 3I) and upregulated the expression of genes involved in αβ T cells (TCRα) and γδ T cells (TCRδ), as well as in T cell toxicity (IFN-γ, granzyme B, perforin

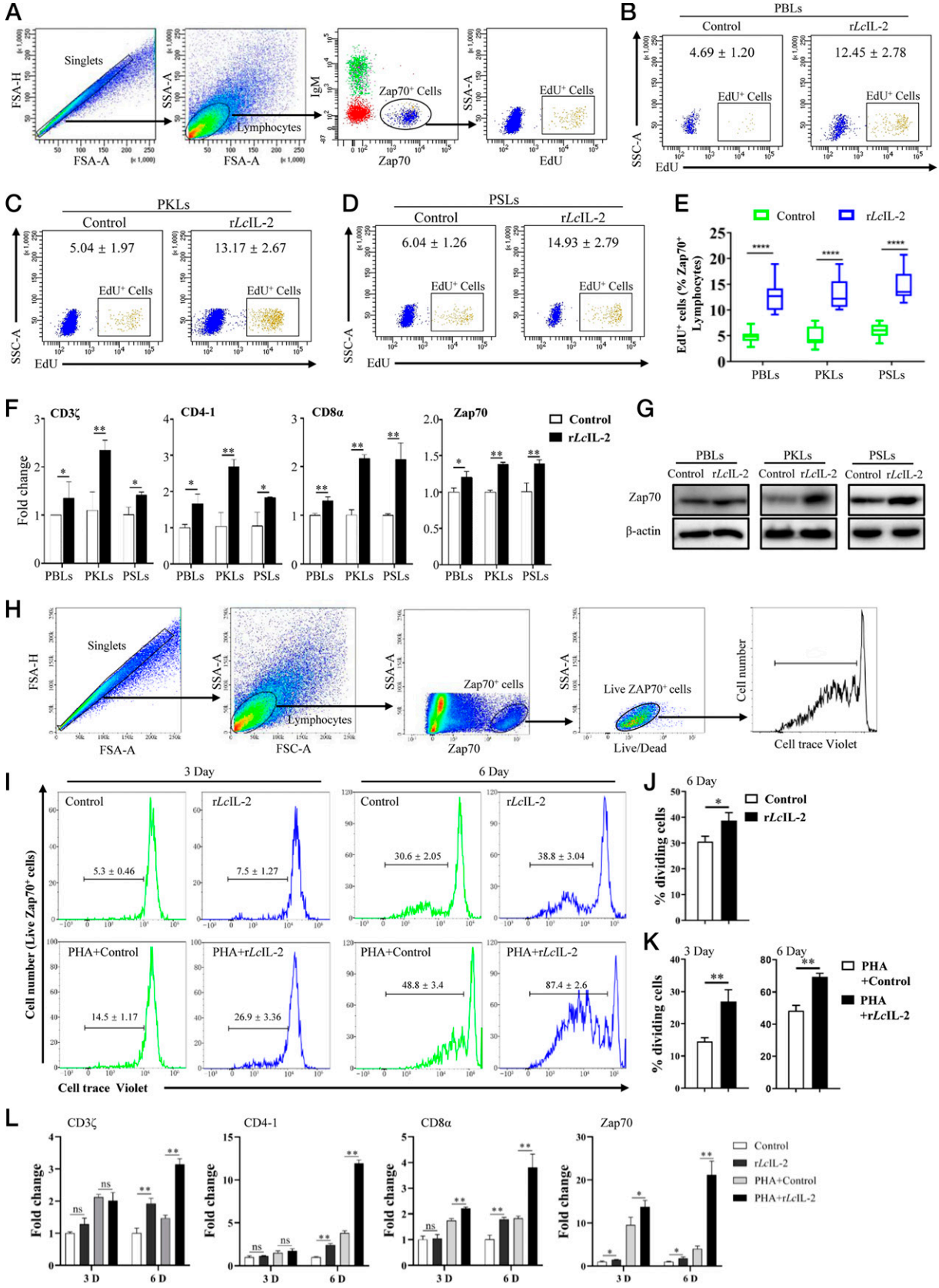

FIGURE 1. IL-2 plays a pivotal role in T cell proliferation in a teleost. (**A**–**G**) T cells ($Zap70^+$ cells) proliferation of PBLs, PKLs, and PSLs from fish stimulated with r*Lc*IL-2 or with BSA for 48 h (control; $n = 15$ fish per group). (A) Gating strategy used to identify proliferating and nonproliferating T cells ($Zap70^+$ cells). (B–D) Flow cytometry scatterplots, showing the percentages of EdU^+ $Zap70^+$ cells in total $Zap70^+$ cells of PBLs (B), PKLs (C), and PSLs (D). (E) Statistical data, showing the percentages of EdU^+ $Zap70^+$ cells in total $Zap70^+$ cells. The expression levels of the T cell marker genes CD3ζ, CD4-1, CD8α, and Zap70 (F) in PBLs, PKLs, and PSLs from fish stimulated with r*Lc*IL-2 or BSA (control), and the protein expression levels of Zap70 (G) in PBLs, PKLs, and PSLs from fish stimulated with r*Lc*IL-2 or BSA (control). (**H**–**L**) Analysis of T cell proliferation in PKLs after *(Figure legend continues)*

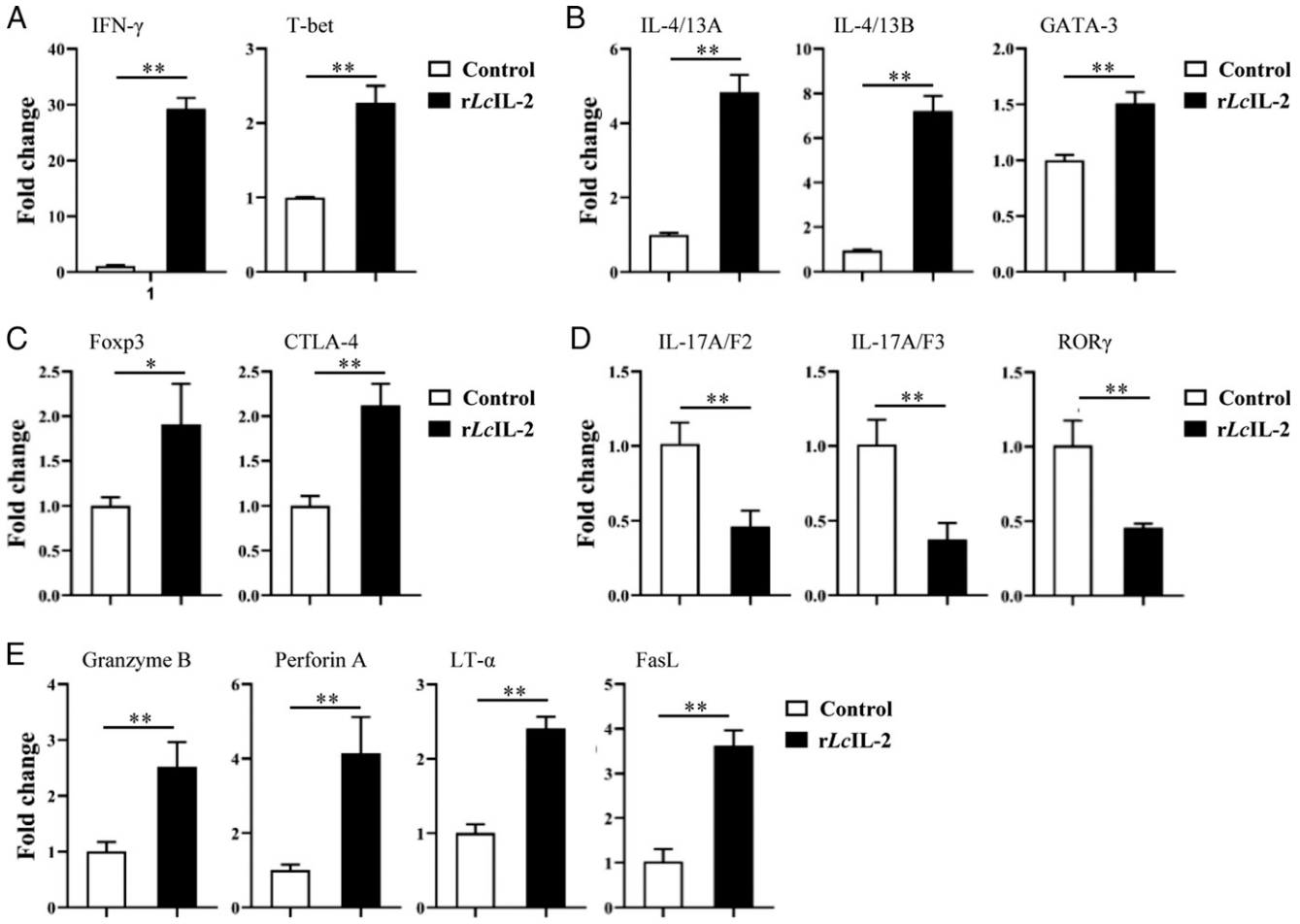

FIGURE 2. IL-2 is involved in T cell differentiation. Gene expression analysis in PKLs after 24 h of stimulation with r*Lc*IL-2 or BSA (control). The expression levels of Th1-associated genes IFN-γ and T-bet (**A**); Th2-associated genes IL-4/13A, IL-4/13B, and GATA3 (**B**); Treg-associated genes Foxp3 and CTLA-4 (**C**); Th17-associated genes IL-17A/F2, IL-17A/F3, and RORγ (**D**); as well as genes associated with the cytotoxic activity of $CD8^+$ T cells: Granzyme B, Perforin A, LT-α, and FasL (**E**). For all genes, relative expression levels were normalized against *Lc*β-actin and expressed as fold change compared with the BSA-stimulated control group at 24 h poststimulation. Bars represent the means of three independent experiments ± SD. All experiments were performed in triplicate. $*p < 0.05$, $**p < 0.01$ (unpaired Student *t* test).

A, LT-α, and FasL) in the infected fish, whereas administration of CsA inhibited the proliferation of T cells and the expression of these genes (Fig. 3J, 3K). It is worth noting that IL-17A/F3 expression was significantly inhibited by *Lc*IL-2 in the *P. plecoglossicida*–infected fish (Supplemental Fig. 2N) but was not influenced by CsA treatment. In addition, 7 d after *P. plecoglossicida* infection, the expression levels of the *P. plecoglossicida* genes *rpoD* and *gyrB* in the fish spleen and head kidney were significantly greater in the CsA-treated fish as compared with the r*Lc*IL-2–treated fish (Fig. 3L), suggesting that *P. plecoglossicida* abundance was also significantly greater in the CsA-treated fish as compared with the *Lc*IL-2–treated fish. Compared with the mortality rate of the untreated infected fish, administration of *Lc*IL-2 significantly reduced the mortality rate of the infected fish, while administration of CsA significantly increased the mortality rate of the infected fish (Fig. 3M). Thus, our results indicated that the *Lc*IL-2–induced T cell response was required for elimination of bacterial infection in the large yellow croaker.

The large yellow croaker possesses an uncanonical IL-2R complex

Because our results showed that *Lc*IL-2 plays a role in T cell proliferation and differentiation, we next investigated the molecular mechanisms underlying those functions. Mammalian IL-2 acts on the target cell via its receptor complex, which is composed of IL-2Rα, IL-2Rβ, and γc (49). Previously, we successfully cloned *Lc*IL-15Rα, *Lc*IL-2Rβ, and *Lc*γc based on the large yellow croaker genome (51). The functional domain organization and tertiary structures of *Lc*IL-2Rβ and *Lc*γc were highly similar to those of their human counterparts (Fig. 4A, 4B). However, *Lc*IL-15Rα, like other teleost IL-15Rα proteins, contains only one sushi domain at the N terminus, while mammalian IL-2Rα contains two sushi domains (Fig. 4A). To

stimulation with r*Lc*IL-2 alone or with r*Lc*IL-2 plus PHA for 3 and 6 d. (H) Gating strategy used to identify proliferating T cells ($Zap70^+$ cells). (I) Representative histograms showing $Zap70^+$ cell proliferation at 3 and 6 d after stimulation with r*Lc*IL-2 alone (upper panel) or with r*Lc*IL-2 plus PHA (lower panel). (J and K) Statistical data, showing the percentages of dividing $Zap70^+$ cells in total $Zap70^+$ cells of PKLs after stimulation with r*Lc*IL-2 alone (J) or with r*Lc*IL-2 plus PHA (K). (L) The expression levels of the T cell marker genes CD3ζ, CD4-1, CD8α, and Zap70 of PKLs after stimulation with r*Lc*IL-2 alone or with r*Lc*IL-2 plus PHA. In all graphs, bars represent the means of three independent experiments ± SD. All experiments were performed in triplicate. $*p < 0.05$, $**p < 0.01$, $***p < 0.001$, $****p < 0.0001$ (unpaired Student *t* test).

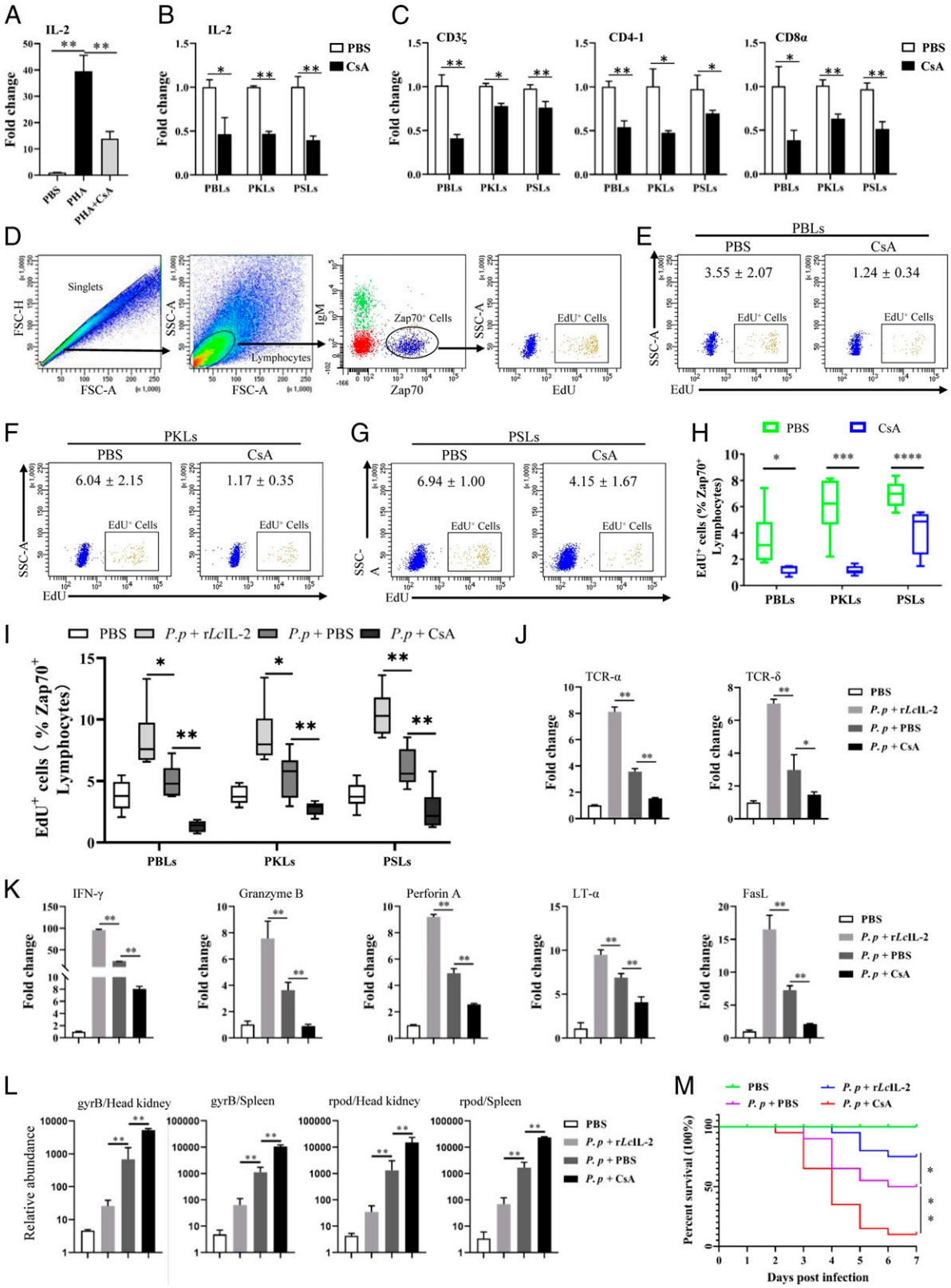

FIGURE 3. IL-2 facilitates T cell–mediated infection elimination in large yellow croaker. (**A**) The expression levels of *Lc*IL-2 in PKLs stimulated with PHA in the presence or absence of CsA for 24 h. (**B**) The expression levels of *Lc*IL-2 in PBLs, PKLs, and PSLs from large yellow croaker treated with CsA or PBS (control; $n = 6$ fish per group). (**C–H**) T cells ($Zap70^+$ cells) proliferation of PBLs, PKLs, and PSLs from large yellow croaker treated with CsA or PBS (control; $n = 6$ fish per group). (C) The expression levels of T cell marker genes CD3ζ, CD4-1, and CD8α. (D) Gating strategy used to identify the proliferation of T cells ($Zap70^+$ cells). (E–G) Flow cytometry scatterplots, showing the percentages of EdU^+ $Zap70^+$ cells in total $Zap70^+$ cells of PBLs (E), PKLs (F), and PSLs (G). (H) Statistical data, showing the percentages of EdU^+ $Zap70^+$ cells in total $Zap70^+$ cells of PBLs, PKLs, and PSLs from normal fish. (**I–M**) Effects of r*Lc*IL-2 or CsA treatment on the immune response to *P. plecoglossicida* (*P. p*) challenge in the large yellow croaker. The blank control group was uninfected (injected with PBS); the negative control group was infected with *P. plecoglossicida* and treated with PBS. (I) Statistical data, showing the percentages of EdU^+ $Zap70^+$ cells in total $Zap70^+$ cells of PBLs, PKLs, and PSLs from the *P. plecoglossicida*–infected *(Figure legend continues)*

determine whether these three receptor subunits were involved in *Lc*IL-2 signaling, we measured their response to *Lc*IL-2 stimulation. We found that the mRNA expression levels of all three subunits (*Lc*IL-15Rα, *Lc*IL-2Rβ, and *Lc*γc) were significantly increased in PKLs in response to r*Lc*IL-2 (Fig. 4C), indicating that these subunits might participate in *Lc*IL-2 signaling.

We next used Co-IP assays to confirm the participation of *Lc*IL-2R subunits in *Lc*IL-2 signaling. We found that *Lc*IL-2 interacted with *Lc*IL-15Rα and *Lc*IL-2Rβ, but not with *Lc*γc (Fig. 4D–F). It has been shown that IL-2R subunits do not preform a stable heterotrimer in the absence of IL-2 in mammals (28). Therefore, we next investigated whether the *Lc*IL-2R subunits formed a heterotrimer in the absence of *Lc*IL-2. Co-IP analyses showed that *Lc*IL-15Rα did not associate with *Lc*IL-2Rβ or *Lc*γc in the absence of *Lc*IL-2, but *Lc*IL-2Rβ was physically associated with *Lc*γc (Fig. 4G–I). However, *Lc*IL-2, *Lc*IL-15Rα, and *Lc*IL-2Rβ formed a stable heterodimer, as did *Lc*IL-2, *Lc*IL-2Rβ, and *Lc*γc (Fig. 4J, 4K). These results led us to propose that *Lc*IL-2 may bind to both *Lc*IL-15Rα and *Lc*IL-2Rβ equally, resulting in the formation of a heterotrimer (*Lc*IL-2/*Lc*IL-15Rα/*Lc*IL-2Rβ), and that *Lc*γC was then recruited by *Lc*IL-2Rβ to form the signal transduction complex *Lc*IL-2/*Lc*IL-15Rα/*Lc*IL-2Rβ/*Lc*γC.

IL-2 initiates JAK–STAT5 signaling to regulate T cell proliferation and differentiation in the large yellow croaker

To further explore the mechanisms by which *Lc*IL-2 regulates T cell proliferation and differentiation, we investigated the *Lc*IL-2–initiated signaling pathway. Because JAK–STAT5 is the intrinsic signaling pathway for the IL-2–mediated T cell response in mammals (49), we investigated the involvement of the JAK–STAT5 pathway, represented by the JAK1, JAK3, STAT5a, and STAT5b molecules, in the *Lc*IL-2–mediated T cell response. JAK1, JAK3, STAT5a, and STAT5b were searched from the large yellow croaker genome database. Notably, the organization, primary structure, and tertiary structure of key functional domains of these molecules were highly similar to their counterparts in human (Supplemental Fig. 1A–D), intimating that the JAK–STAT5 signaling pathway might be conserved across vertebrates such as fish and mammals.

To specifically investigate how *Lc*IL-2 regulates downstream signaling, we examined the interactions of key signaling molecules in the JAK–STAT5 pathway with the cytoplasmic tails of *Lc*IL-2Rβ and *Lc*γc, which contain the predicted signaling motifs that may transduce signals to the cytoplasm (51). Co-IP analyses showed that *Lc*IL-2Rβ interacted with JAK1, and that *Lc*γc interacted with JAK3 (Fig. 5A, 5B). Both STAT5a and STAT5b interacted with *Lc*IL-2Rβ, but neither interacted with *Lc*γc (Fig. 5C–F). These results suggested that *Lc*IL-2Rβ might be especially important for *Lc*IL-2 signaling. Notably, the mRNA expression levels of JAK1/3 and STAT5a/b increased significantly in response to r*Lc*IL-2 stimulation (Fig. 5G), as did the phosphorylation of STAT5a/b (Fig. 5H). Indeed, after 30 min of r*Lc*IL-2 stimulation, elevated STAT5a/b phosphorylation was observed in PKL nuclei (Fig. 5I). These results suggested that *Lc*IL-2 may activate the JAK–STAT5 signaling pathway.

Consistent with this suggestion, subsequent blockade of STAT5a/b using the specific inhibitor STAT5-IN-1 reduced the *Lc*IL-2–induced increase in STAT5a/b phosphorylation (Fig. 5J). *Lc*IL-2–induced T cell proliferation was also reduced because of this inhibition of STAT5a/b phosphorylation (Fig. 5K–M), as was the *Lc*IL-2–induced upregulation of genes associated with T cell differentiation (Fig. 5N). Collectively, these observations indicated that *Lc*IL-2 activated the conserved JAK–STAT5 signaling pathway to regulate T cell immunity in the large yellow croaker.

The MAPK and mTORC1 axes are critical for IL-2–regulated T cell proliferation and differentiation in the large yellow croaker

MAPK/Erk signaling is implicated in IL-2–mediated T cell proliferation and differentiation in mammals (49). To determine whether the MAPK/Erk signaling pathways similarly participate in *Lc*IL-2–mediated T cell proliferation and differentiation, we investigated key components of the MAPK axis: Mek1/2 and Erk1/2. The organization, primary structure, and tertiary structure of large yellow croaker Mek1/2 and Erk1/2 were highly similar to their human homologs (Supplemental Fig. 1E–H). Mek1/2 and Erk1/2 were significantly upregulated in response to r*Lc*IL-2 stimulation (Fig. 6A), suggesting their role in *Lc*IL-2–mediated signaling. Because the phosphorylation of Mek1/2 and Erk1/2 is crucial for MAPK/Erk signaling activation and downstream function, we examined the phosphorylation of these proteins in response to r*Lc*IL-2 stimulation in the large yellow croaker. Mek1/2 and Erk1/2 phosphorylation, but not total protein content, was noticeably increased in PKLs after r*Lc*IL-2 stimulation as compared with resting cells (Fig. 6B). Indeed, elevated Mek1/2 and Erk1/2 phosphorylation in the cytoplasm of PKLs was obvious after 30 min of r*Lc*IL-2 stimulation (Fig. 6C, 6D). These results again suggested that MAPK/Erk signaling was activated in the PKLs in response to r*Lc*IL-2 stimulation.

Consistent with this supposition, the blockade of Erk1/2 with the specific inhibitor SHC772984 before *Lc*IL-2 stimulation reduced the *Lc*IL-2–induced enhancement of Erk1/2 phosphorylation (Fig. 6E). *Lc*IL-2–induced T cell proliferation was also impaired after Erk1/2 inhibition (Fig. 6F–H), as was the *Lc*IL-2–regulated expression of genes associated with T cell differentiation (Fig. 6I). Collectively, these observations suggested that MAPK/Erk signaling was crucial for *Lc*IL-2–induced T cell proliferation and differentiation in the large yellow croaker.

Another important serine/threonine kinase for IL-2 signal transduction is mTOR (49). In mammals, mTOR is the central molecule in two different kinase complexes: mTORC1 and mTORC2 (52, 53). Mammalian mTORC1 has been implicated in IL-2–mediated T cell immunity (52). Because mTOR in the large yellow croaker is highly similar to mammalian mTOR with respect to functional domain organization, tertiary structure, and overall conformation (Supplemental Fig. 1I, 1J), we explored the involvement of large yellow croaker mTORC1 in *Lc*IL-2 signaling. The mRNA expression levels of mTOR and AKT (upstream of mTORC1) increased significantly in response to *Lc*IL-2 stimulation, while 4E-BP1 (downstream of mTORC1) was unaffected (Fig. 7A). AKT, mTOR, and 4E-BP1 phosphorylation, but not total protein content, was markedly increased in PKLs after up to 45 min of r*Lc*IL-2 stimulation (Fig. 7B, 7C). Indeed, the elevated phosphorylation of mTOR and 4E-BP1 in the PKLs was obvious after 30 min of *Lc*IL-2 stimulation (Fig. 7D, 7E). These results suggested that the mTORC1 axis plays a role in *Lc*IL-2 signaling.

Consistent with this supposition, the inhibition of mTORC1 with the specific inhibitor rapamycin before *Lc*IL-2 stimulation severely impaired the *Lc*IL-2–induced phosphorylation of 4E-BP1 (Fig. 7F),

fish. (J) Relative expression of T cell marker genes TCRα and TCRδ upon r*Lc*IL-2 or CsA treatment in the *P. plecoglossicida*–infected fish ($n = 3$ fish per group). (K) Relative expression of genes involved in T cell toxicity in the fish spleen on day 7 postinfection ($n = 3$ fish per group). (L) Relative expression of *P. plecoglossicida* genes (as a proxy for *P. plecoglossicida* abundance) 7 d postinfection ($n = 3$ fish per group). (M) Kaplan–Meier survival curves for the four treatment groups ($n = 50$ per group). In all histograms, bars represent the means of three independent experiments ± SD. All experiments were performed in triplicate. $^{*}p < 0.05$, $^{**}p < 0.01$, $^{***}p < 0.001$, $^{****}p < 0.0001$ (unpaired Student *t* test).

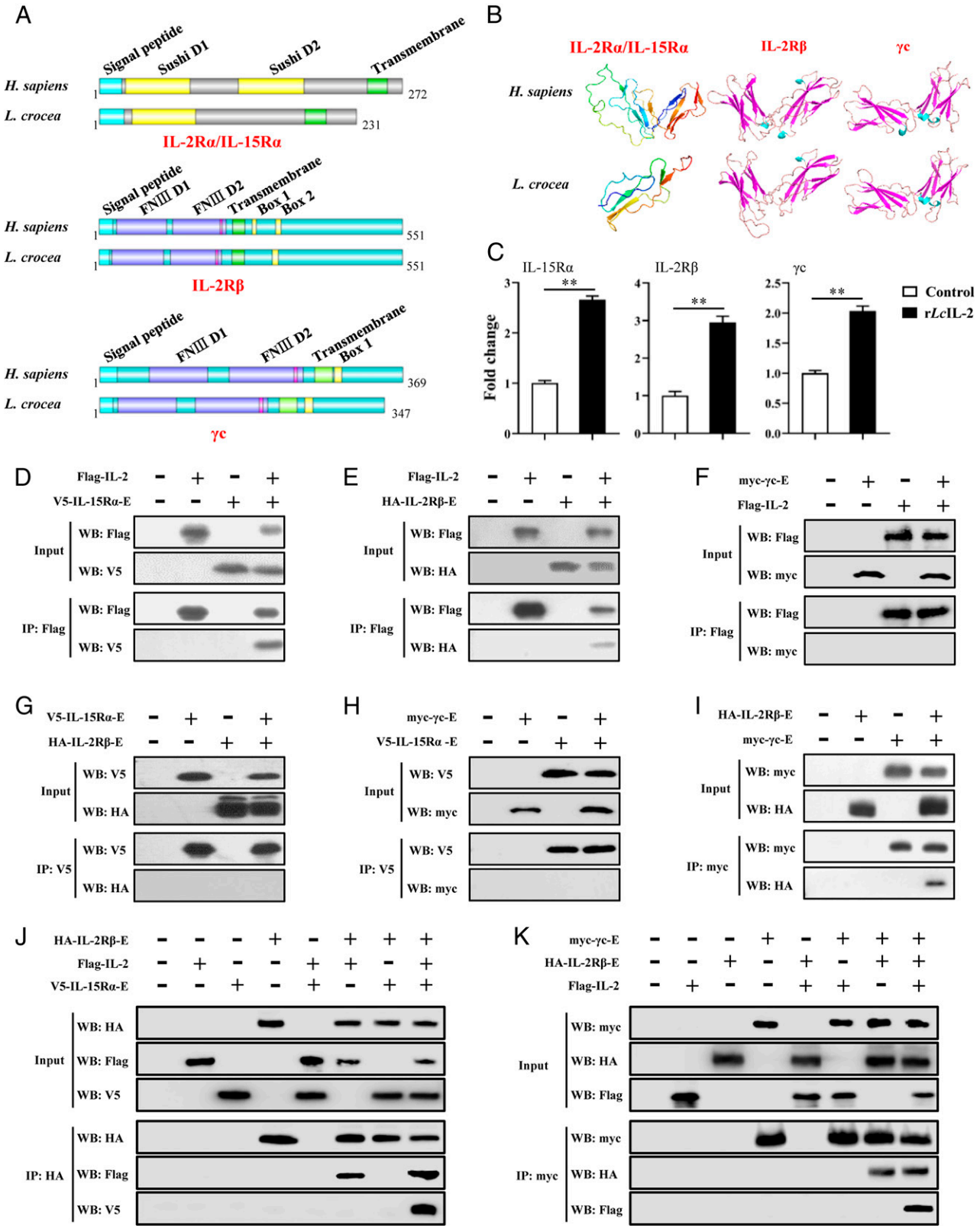

FIGURE 4. The large yellow croaker possesses an uncanonical IL-2R complex. (**A**) The domain organization of IL-2R subunits in the large yellow croaker and human. (**B**) SWISS-MODEL predictions of the tertiary structures of IL-2R subunits from the large yellow croaker and human. (**C**) The expression levels of *Lc*IL-2R subunits in PKLs after 24-h stimulation with r*Lc*IL-2 or BSA (control). Bars represent the means of three independent experiments ± SD. $*p < 0.05$, $**p < 0.01$ (unpaired Student *t* test). (**D**–**K**) Western blots showing Co-IP assay results. After cotransfection of HEK-293 T cells with the indicated plasmids, Western blot analyses were performed using the indicated Abs directly for input control or after immunoprecipitation with agarose beads. Blots show the following potential interactions: *Lc*IL-2 and *Lc*IL-15Rα (D), *Lc*IL-2 and *Lc*IL-2Rβ (E), *Lc*IL-2 and *Lc*γc (F), *Lc*IL-15Rα and *Lc*IL-2Rβ (G), *Lc*IL-15Rα and *Lc*γc (H), *Lc*IL-2Rβ and *Lc*γc (I), the *Lc*IL-2 complex with *Lc*IL-15Rα and *Lc*IL-2Rβ (J), and the *Lc*IL-2 complex with *Lc*IL-2Rβ and *Lc*γc (K). All experiments were performed in triplicate.

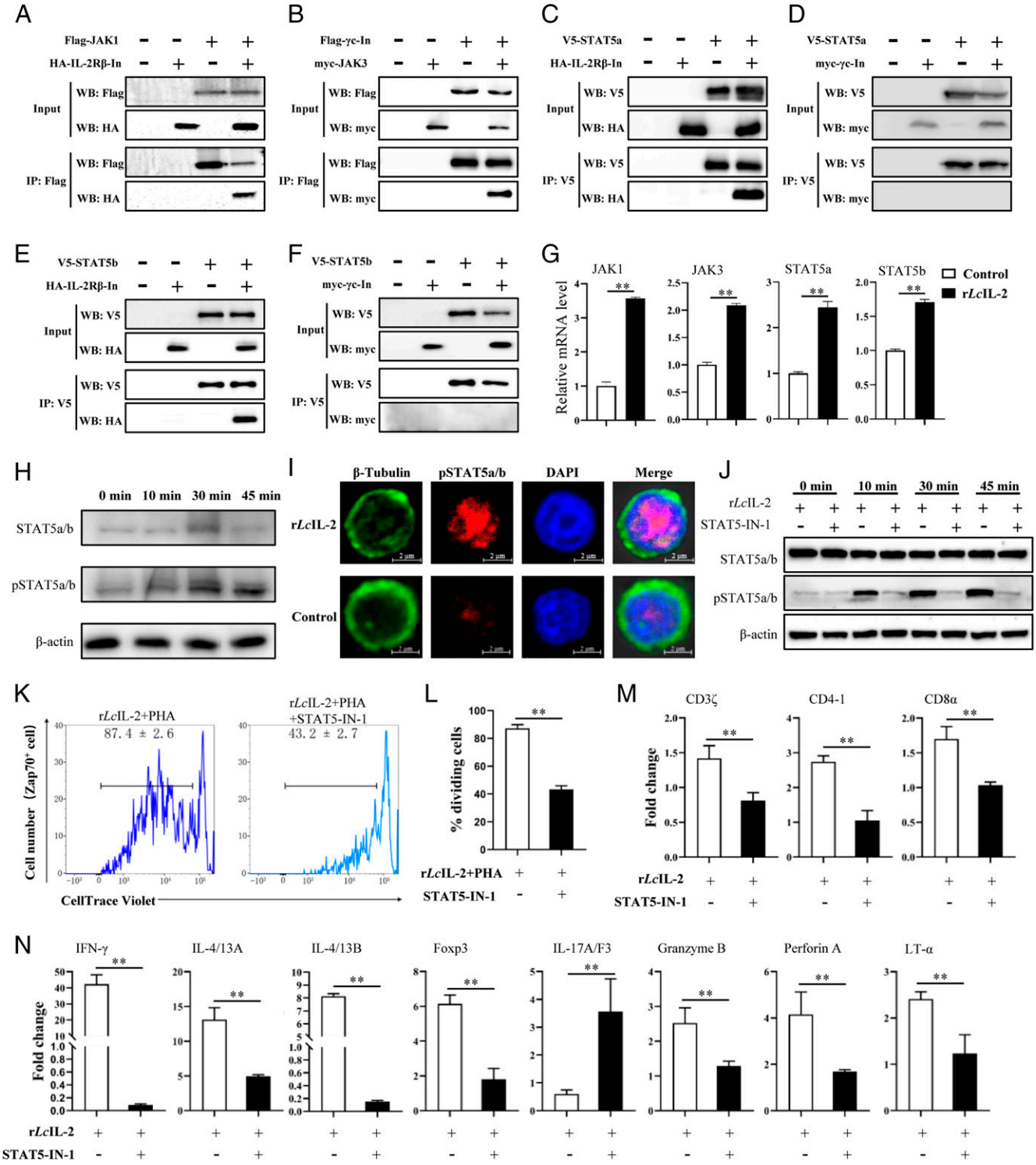

FIGURE 5. IL-2 initiates JAK–STAT5 signaling to regulate T cell proliferation and differentiation in the large yellow croaker. (**A**–**F**) Western blots showing Co-IP assay results. After cotransfection of HEK-293 T cells with the indicated plasmids, Western blot analyses were performed using the indicated Abs directly for input control or after immunoprecipitation with agarose beads. Blots show the following potential interactions: (A) *Lc*IL-2Rβ and JAK1, (B) *Lc*γc and JAK3, (C) *Lc*IL-2Rβ and STAT5a, (D) *Lc*γc with STAT5a, (E) *Lc*IL-2Rβ and STAT5b, and (F) *Lc*γc with STAT5b. (**G**) The expression levels of JAK1/3 and STAT5a/b in PKLs after 24-h stimulation with r*Lc*IL-2 or BSA (control). (**H**) Western blots showing STAT5a/b protein expression and phosphorylation after up to 45 min of r*Lc*IL-2 stimulation. (**I**) Immunofluorescence analysis showing STAT5a/b phosphorylation after 30 min of r*Lc*IL-2 stimulation. (**J**–**N**) Effects of pretreatment with the STAT5a/b inhibitor STAT5-IN-1 on STAT5a/b in PKLs stimulated with r*Lc*IL-2 or r*Lc*IL-2+PHA. (J) Western blots showing STAT5a/b protein expression and phosphorylation after up to 45 min of r*Lc*IL-2 stimulation. (K) Representative histograms showing $Zap70^+$ cells proliferation. (L) Statistical data, showing the percentages of dividing $Zap70^+$ cells at 6 d poststimulation. (M) The expression levels of the T cell marker genes CD3ζ, CD4-1, and CD8α in PKLs after 24-h stimulation. (N) The expression levels of representative Th1-, Th2-, Treg-, Th17-, and cytotoxic T cell–associated genes after 24 h of stimulation. In all histograms, bars represent the means of three independent experiments ± SD. All experiments were performed in triplicate. $*p < 0.05$, $**p < 0.01$ (unpaired Student *t* test).

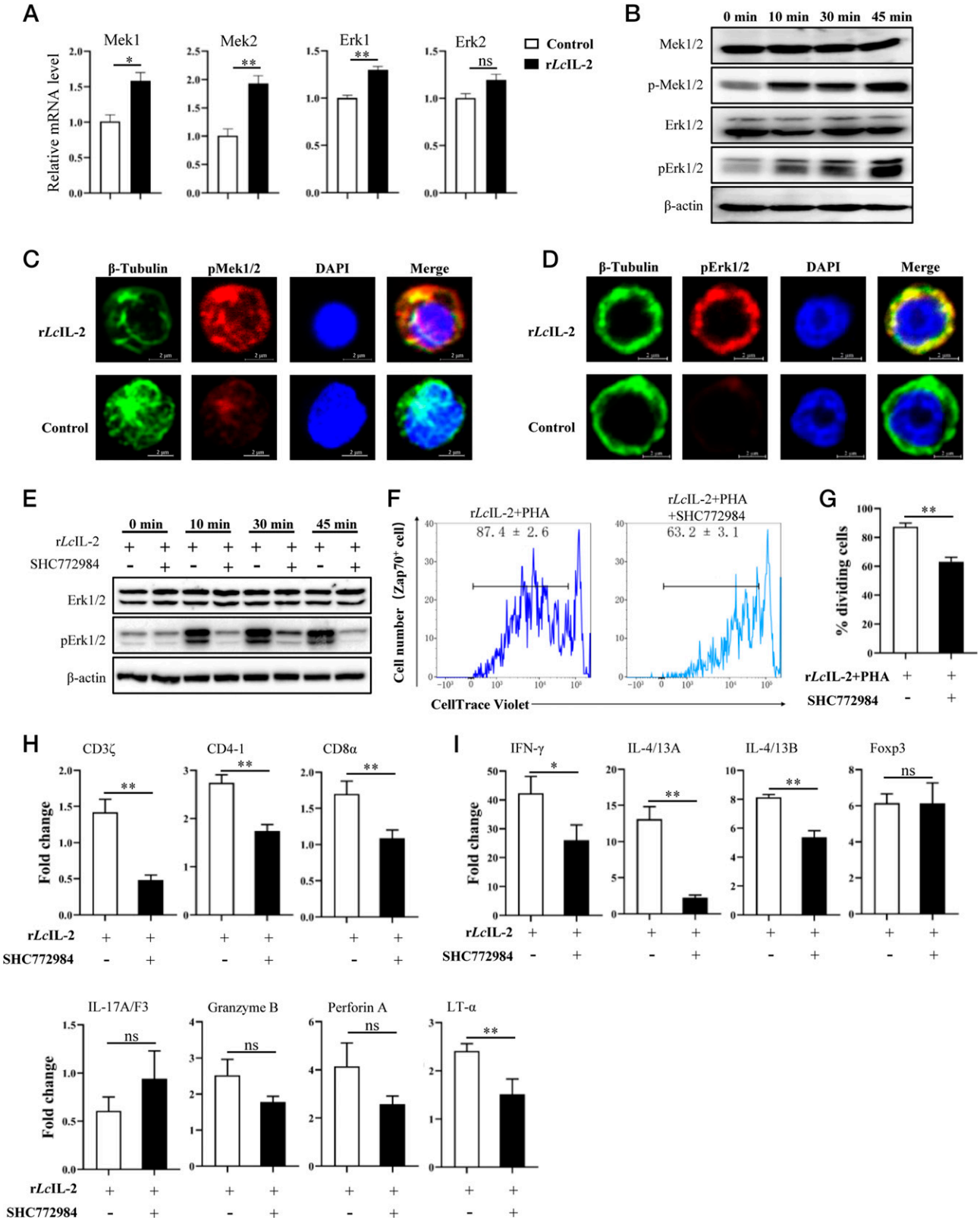

FIGURE 6. The MAPK/Erk axis is critical for IL-2–regulated T cell proliferation and differentiation in large yellow croaker. (**A**) The expression levels of Mek1/2 and Erk1/2 in PKLs after 24-h stimulation with r*Lc*IL-2 or BSA (control). (**B**) Western blot analysis showing protein and phosphorylation levels after up to 45 min of r*Lc*IL-2 stimulation. (**C** and **D**) Representative immunofluorescence analysis showing phosphorylation of Mek1/2 (C) and Erk1/2 (D) after 30 min of r*Lc*IL-2 stimulation. (**E–I**) Effects of pretreatment with the Erk1/2 inhibitor SCH772984 on Erk1/2 in PKLs stimulated with r*Lc*IL-2 or r*Lc*IL-2+PHA. (E) Western blots showing Ekr1/2 protein expression and phosphorylation after up to 45 min of r*Lc*IL-2 stimulation. (F) Representative histograms showing $Zap70^+$ cell proliferation. (G) Statistical data, showing the percentages of dividing $Zap70^+$ cells at 6 d poststimulation. (H) The expression levels of the T cell marker genes CD3ζ, CD4-1, and CD8α in PKLs after 24-h stimulation. (I) The expression levels of representative Th1-, Th2-, Treg-, Th17-, and cytotoxic T cell–associated genes after 24 h of stimulation. In all histograms, bars represent the means of three independent experiments ± SD. All experiments were performed in triplicate. $*p < 0.05$, $**p < 0.01$ (unpaired Student *t* test).

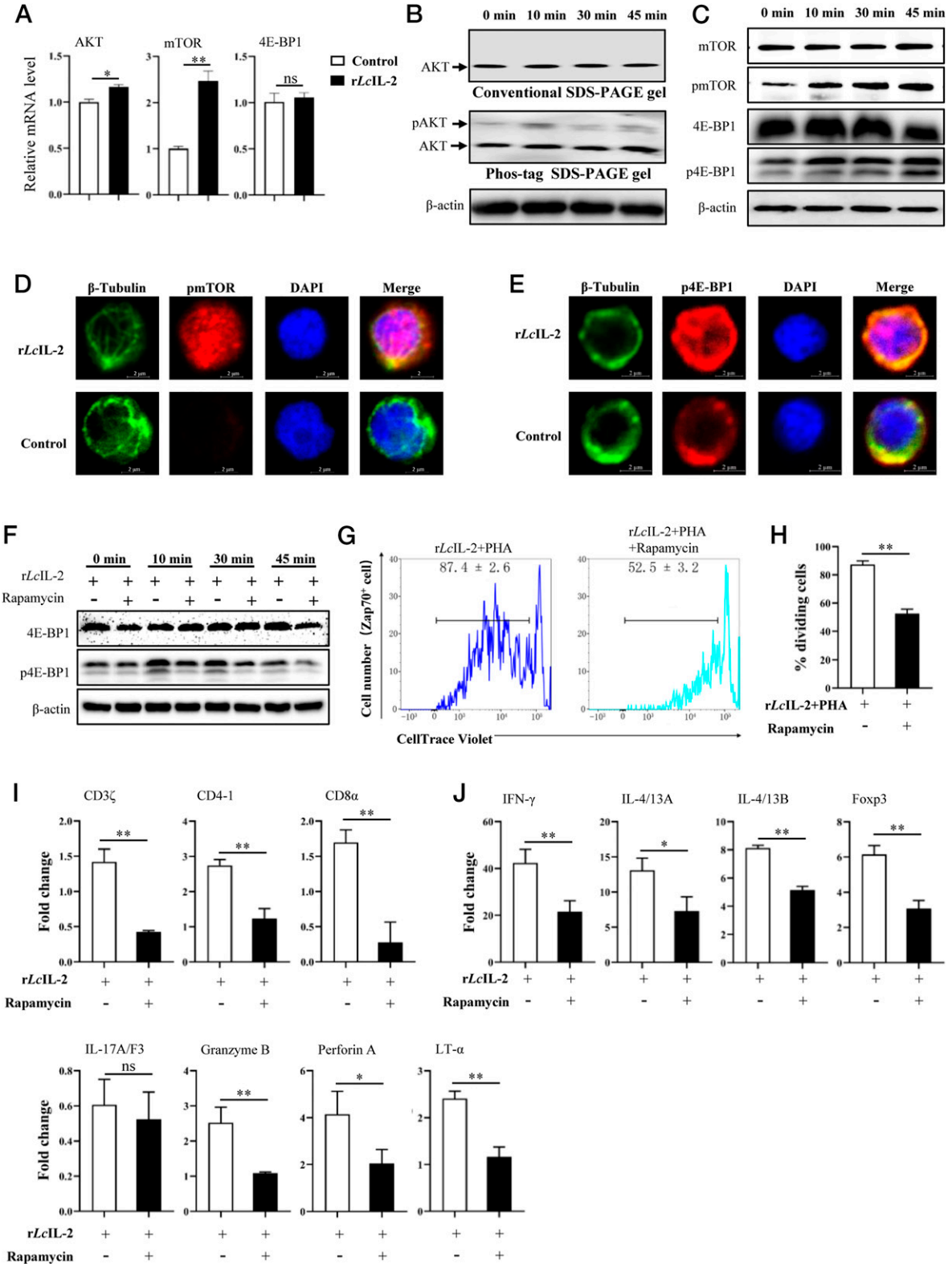

FIGURE 7. The mTORC1 axis is required for IL-2–regulated T cell proliferation and differentiation in the large yellow croaker. (**A**) The expression levels of AKT, mTOR, and 4E-BP1 in PKLs after 24-h simulation with r*Lc*IL-2 or BSA (control). (**B**) Western blot analysis of Phos-tag SDS-PAGE gels, showing protein and phosphorylation levels of AKT after up to 45 min of r*Lc*IL-2 stimulation. (**C**) Western blot analysis showing protein and phosphorylation levels of mTOR and 4E-BP1 after up to 45 min of r*Lc*IL-2 stimulation. (**D** and **E**) Representative immunofluorescence analysis showing phosphorylation of mTOR (D) and 4E-BP1 (E) after 30 min of r*Lc*IL-2 stimulation. (**F–J**) Effects of pretreatment with the mTORC inhibitor rapamycin on the mTORC1 axis in PKLs stimulated with r*Lc*IL-2 or r*Lc*IL-2+PHA. (F) Western blots showing 4E-BP1 protein expression and phosphorylation after up to 45 min of r*Lc*IL-2 stimulation. (G) Representative histograms showing $Zap70^+$ cell proliferation. (H) Statistical data, showing the percentages of dividing $Zap70^+$ cells at 6 d poststimulation. (I) The expression levels of the T cell marker genes CD3ζ, CD4-1, and CD8α after 24-h stimulation. (J) The expression levels of representative Th1-, Th2-, Treg-, Th17-, and cytotoxic T cell–associated genes after 24 h of stimulation. In all histograms, bars represent the means of three independent experiments ± SD. All experiments were performed in triplicate. $*p < 0.05$, $**p < 0.01$ (unpaired Student *t* test).

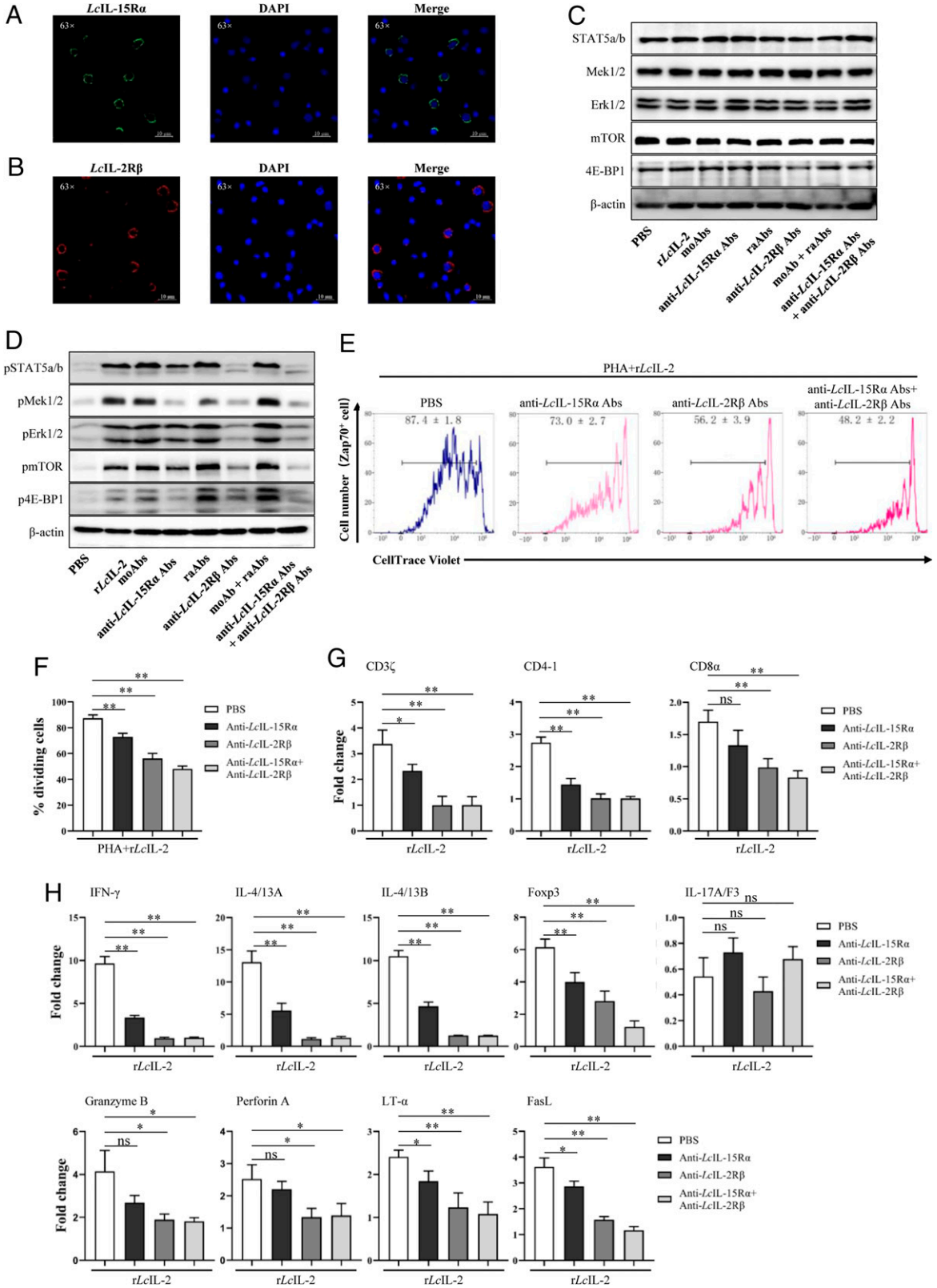

FIGURE 8. IL-2 modulates T cell proliferation and differentiation through its receptor complex in the large yellow croaker. (**A** and **B**) Immunofluorescence micrographs showing *Lc*IL-15Rα$^+$ lymphocytes (A) labeled with anti–*Lc*IL-15Rα Abs and (B) *Lc*IL-2Rβ$^+$ lymphocytes labeled with anti–*Lc*IL-2Rβ Abs. (**C**–**H**) Analysis of PKLs incubated with anti–*Lc*IL-15Rα and/or anti–*Lc*IL-2Rβ, followed by stimulation with r*Lc*IL-2; control groups were incubated with PBS, r*Lc*IL-2 alone, or nonspecific mouse Abs (moAbs) and/or nonspecific rabbit Abs (raAbs) prior to r*Lc*IL-2 or r*Lc*IL-2+PHA stimulation. (C and D) Western blots showing total protein (C) and phosphorylation (D) of STAT5a/b, Mek1/2, Erk1/2, mTOR, and 4E-BP1 after 30 min of r*Lc*IL-2 stimulation. (E) Representative histograms showing Zap70$^+$ cell proliferation at 6 d poststimulation. (F) Statistical data, showing the percentages of dividing Zap70$^+$ cells at 6 d poststimulation. (G) The expression levels of the T cell marker genes CD3ζ, CD4-1, and CD8α after 24 h of r*Lc*IL-2 stimulation. (H) The expression levels of representative Th1-, Th2-, Treg-, Th17-, and cytotoxic T cell–associated genes after 24 h of r*Lc*IL-2 stimulation. In all histograms, bars represent the means of three independent experiments ± SD. All experiments were performed in triplicate. *$p < 0.05$, **$p < 0.01$ (unpaired Student *t* test).

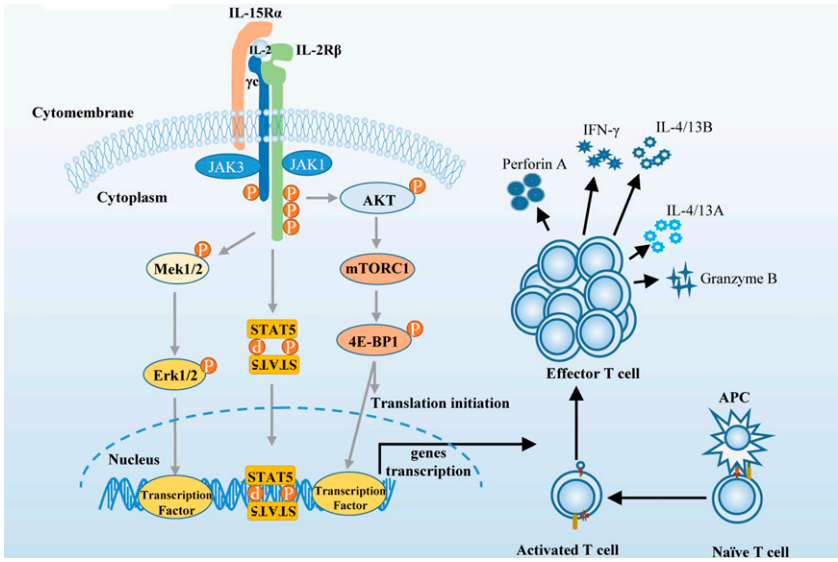

FIGURE 9. Canonical IL-2 signaling couples MAPK/Erk and mTORC1 to regulate ancestral T cell immunity in fish. In the large yellow croaker, *Lc*IL-2 may bind to both *Lc*IL-15Rα and *Lc*IL-2Rβ equally, resulting in the formation of a heterotrimer (*Lc*IL-2/*Lc*IL-15Rα/*Lc*IL-2Rβ), and that *Lc*γC was then recruited by *Lc*IL-2Rβ to form the signal transduction complex *Lc*IL-2/*Lc*IL-15Rα/*Lc*IL-2Rβ/*Lc*γC. This complex may then activate the conserved STAT5-dependent JAK–STAT signaling pathway, as well as the MAPK/Erk and mTORC1 signaling pathways. These three signaling pathways may then synergistically regulate the expression of genes involved in T cell proliferation, differentiation, and function, thus modulating T cell immunity.

demonstrating that rapamycin effectively inhibited *Lc*IL-2–induced mTORC1 signaling. *Lc*IL-2–induced T cell proliferation was also impaired after mTORC1 inhibition (Fig. 7G–I), as was the *Lc*IL-2–regulated expression of genes associated with T cell differentiation (Fig. 7J). Collectively, these results suggested that mTORC1 signaling is required for *Lc*IL-2–mediated T cell activation in the large yellow croaker.

IL-2 modulates T cell proliferation and differentiation though its receptor complex

Given γc serves as a common receptor for γc cytokine family members in mammals (54), we next explored the participation of *Lc*IL-15Rα and *Lc*IL-2Rβ in IL-2 signaling by blocking *Lc*IL-15Rα and/or *Lc*IL-2Rβ with the polyclonal Abs anti–*Lc*IL-15Rα and anti–*Lc*IL-2Rβ designed for this study. Western blots showed that the affinity-purified anti–*Lc*IL-15Rα and anti–*Lc*IL-2Rβ polyclonal Abs bound specifically to endogenous *Lc*IL-15Rα and *Lc*IL-2Rβ in the head kidney and spleen, respectively; no cross-reactivity was observed (data not shown). Consistent with this, immunofluorescence analysis showed that anti–*Lc*IL-15Rα and anti–*Lc*IL-2Rβ specifically recognized the corresponding molecules expressed on PKLs (Fig. 8A, 8B).

Blockade with normal mouse and/or rabbit Abs had no effect on the r*Lc*IL-2–stimulated phosphorylation of STAT5a/b, Mek1/2, Erk1/2, mTOR, and 4E-BP1 in PKLs (Fig. 8C, 8D). However, the r*Lc*IL-2–stimulated phosphorylation of these proteins was reduced when *Lc*IL-15Rα or *Lc*IL-2Rβ was blockaded with the specific anti–*Lc*IL-15Rα polyclonal Ab or the specific anti–*Lc*IL-2Rβ polyclonal Ab, respectively (Fig. 8C, 8D). When both *Lc*IL-15Rα and *Lc*IL-2Rβ were blockaded, the r*Lc*IL-2–stimulated phosphorylation of STAT5a/b, Mek1/2, Erk1/2, mTOR, and 4E-BP1 was almost completely inhibited (Fig. 8C, 8D). *Lc*IL-2–induced T cell proliferation was also suppressed by the Ab-driven blockade of *Lc*IL-15Rα, *Lc*IL-2Rβ, or both (Fig. 8E–G). The blockade of *Lc*IL-15Rα and/or *Lc*IL-2Rβ also weakened the regulatory effects of *Lc*IL-2 on T cell–associated gene expression in PKLs (Fig. 8H). Thus, our results suggested that *Lc*IL-2 activates the pathways associated with the JAK–STAT5, MAPK, and mTORC1 axes via its receptor complex *Lc*IL-15Rα/*Lc*IL-2Rβ/*Lc*γc (Fig. 9).

Discussion

The vertebrate immune system is composed of a variety of immune cells that are distributed throughout the body of the host, and the development of mechanisms that enable efficient cell–cell communication was therefore critical for the evolution of this complex immune system (55). One such communication mechanism is mediated by an array of secreted factors collectively termed cytokines (56). Cytokines, which are widely distributed, highly efficient, and functionally pleiotropic, are critically important for the delicate coordination of different immune cells in response to pathogen invasion. T cell immunity processes, including activation by an APC, the differentiation and functioning of effector T cells, and the activation of cognate B cells, also rely on cytokines (8). One of the most well-known cytokines, IL-2, is mainly produced by activated $CD4^+$ T cells; IL-2 plays crucial roles in the promotion of $CD4^+$ and $CD8^+$ T cell proliferation, the regulation of $CD4^+$ T cell differentiation, and the mediation of the cytolytic activity of $CD8^+$ T cells (18, 19, 57–59). Although IL-2 homologs have been identified in several fish species (42, 60–62), details of the regulatory roles played by IL-2 in T cell immunity remain largely unclear in teleosts. In this study, we demonstrated that *Lc*IL-2 enhanced T cell proliferation and modulated T cell differentiation. Because we still cannot visually distinguish T cell subsets in the large yellow croaker as the lack of effective Abs, we have detected the marker gene expression to reflect the function of *Lc*IL-2 in T cell differentiation. Gene expression analyses suggested that *Lc*IL-2 induced the differentiation of $CD8^+$ T cells into effector cytotoxic T cells; facilitated the differentiation of $CD4^+$ T cells into Th1, Th2, and Treg cells; and inhibited the differentiation of $CD4^+$ T cell into Th17. Although the use of gene expression to follow the immune response has inherent limitations, our results have provided valuable evidence to clarify the roles played by IL-2 in T cell response in teleosts. However, further study is needed to elucidate the roles of *Lc*IL-2 in regulating the differentiation of Th cell subsets.

IL-2 signaling is required for the development of Th1 and $CD8^+$ T cells, which are crucial for host defense against pathogens in mammals (18, 58). Recent studies show that IL-2 induced the expression of Th1-secreted IFN-γ in several fish species (61–64). Consistent with this, we found that *Lc*IL-2 promoted T cell expansion, upregulated genes associated with Th1 and $CD8^+$ cytotoxic T cells, and facilitated the elimination of invading bacterial pathogens in the large yellow croaker. Importantly, these beneficial effects disappeared when *Lc*IL-2 production was suppressed by CsA, and fish treated with CsA were more susceptible to *P. plecoglossicida* infection. In both mammals and teleosts, Th1 T cells and cytotoxic $CD8^+$ T cells play important roles in the eradication of

extracellular pathogenic bacteria (41, 65, 66). Therefore, we speculated that IL-2–mediated elimination of invaded bacteria may result from the protective Th1 and $CD8^+$ cytotoxic T cell immunity in this species. Although the inhibition of *Lc*IL-2 production by the immunosuppressive drug CsA cannot exclude confounding effects from other cell lineages and cytokines, our results nonetheless provide intriguing insights into the possible roles played by IL-2 in the T cell–mediated clearance of invading bacteria in teleosts. In future studies, IL-2–knockout models using CRISPR-Cas9 is expected to further clarify the IL-2–mediated regulation of T cell–associated immunity in teleosts.

The mechanisms underlying IL-2–regulated T cell proliferation, differentiation, and function have been well characterized in mammals (49). In mammals, the IL-2 activation of STAT5-mediated transcriptional programs is undoubtedly key to the biological activities of IL-2 (49). For example, IL-2–stimulated peripheral T cell proliferation is eliminated in STAT5a/b-knockout mice (67). It has also been shown that, primarily via STAT5, IL-2 inhibits IL-17A/F and induces IFN-γ, IL-4, T-bet, GATA3, Foxp3, and CTLA-4 in humans and mice (19, 49, 59, 67). *Lc*IL-2 stimulation also affected the expression of these genes in the large yellow croaker. In addition, the phosphorylation of STAT5a/b was markedly increased in PKLs after r*Lc*IL-2 stimulation, suggesting that *Lc*IL-2 activates the conserved STAT5-dependent JAK–STAT signaling pathway. Consistent with this supposition, blockade of STAT5a/b with the specific inhibitor STAT5-IN-1 severely reduced *Lc*IL-2–induced T cell proliferation and weakened *Lc*IL-2–mediated effects on the expression of related genes. *Lc*IL-2 also triggered the MAPK/Erk axis to promote T cell proliferation and differentiation in the large yellow croaker. In mammals, IL-2 production depends on TCR-initiated MAPK/Erk signaling, suggesting the existence of a positive feedback loop between TCR- and IL-2–mediated signaling (17). Our results suggested that this positive feedback loop may be conserved across mammals and fish and may facilitate the rapid proliferation of T cells in response to pathogen invasion. Finally, mTORC1 signaling was also required for *Lc*IL-2–driven T cell proliferation and differentiation in the large yellow croaker. Indeed, it has been shown that TCR-activated mTORC1 signaling directs effector T cell function by controlling metabolic programming in fish (68). Thus, mTORC1 signaling is crucial for both the IL-2– and the TCR-mediated T cell response. Our results suggested that IL-2 signaling in fish might integrate MAPK/Erk and mTORC1 axes, which are also involved in TCR signaling, to modulate T cell response. This link between TCR and IL-2 signaling in fish highlights the sophistication of the network regulating T cell response in lower vertebrate.

Mammalian IL-2 regulates the functions of various T cells by binding to the high-affinity trimeric IL-2R (49, 57). IL-2Rα acts as a carrier, increasing the affinity of IL-2R for its ligand, while both IL-2Rβ and γc conduct signals to the cytoplasm via their cytoplasmic tails, which contain signaling motifs (27, 69). Three potential IL-2R subunits, IL-15Rα, IL-2Rβ, and γc, have been identified in several bony fish, including the large yellow croaker, grass carp, and rainbow trout (62, 70–73). In this study, *Lc*IL-15Rα, a mammalian IL-2Rα homolog, was incapable of transducing signals because of its short cytoplasmic domain. However, this subunit was required for *Lc*IL-2–mediated T response: when *Lc*IL-15Rα was blocked using a specific Ab, the *Lc*IL-2–activated JAK–STAT5, MAPK, and mTORC1 signals were suppressed, and *Lc*IL-2–regulated expression of certain genes was weakened. In addition, the intercellular regions of *Lc*IL-2Rβ and *Lc*γc bound JAK1 and JAK3, respectively, while *Lc*IL-2Rβ bound STAT5a and STAT5b, demonstrating that *Lc*IL-2Rβ and *Lc*γc are irreplaceable components of the *Lc*IL-2–mediated JAK–STAT5 signaling pathway. Furthermore, the Ab-mediated blockage of *Lc*IL-2Rβ or both *Lc*IL-15Rα and *Lc*IL-2Rβ almost completely eliminated the *Lc*IL-2–driven activation of the JAK–STAT5, MAPK/Erk, and mTORC1 pathways and inverted the expression profiles of *Lc*IL-2–regulated genes associated with T cell function. These results emphasized the critical role of *Lc*IL-2Rβ in IL-2 signaling transduction in the large yellow croaker. Based on our results, we propose that *Lc*IL-2 may activate intercellular signaling through the *Lc*IL-15Rα/*Lc*IL-2Rβ/*Lc*γc heterotrimer complex.

In summary, we demonstrated that *Lc*IL-2 promotes T cell proliferation, modulates T cell differentiation, and is indispensable for T cell–mediated bacterial infection clearance. As an early vertebrate, the large yellow croaker possesses the uncanonical IL-2R complex *Lc*IL-15Rα/*Lc*IL-2Rβ/*Lc*γc, via which *Lc*IL-2 initiates the JAK–STAT5 signal pathway to regulate T cell proliferation, differentiation, and biological function (Fig. 9). More importantly, the *Lc*IL-2 signal couples the MAPK/Erk and mTORC1 axes to modulate T cell response (Fig. 9). Thus, this study comprehensively revealed the signal pathways by which IL-2 regulates T cell response in a teleost. Our results help to clarify the regulatory mechanisms underlying the role of cytokine signaling in teleost T cell response and therefore fill an important gap in our understanding of the evolution of the adaptive immune system.

Disclosures

The authors have no financial conflicts of interest.

References

1. Bonilla, F. A., and H. C. Oettgen. 2010. Adaptive immunity. *J. Allergy Clin. Immunol.* 125(2 Suppl. 2): S33–S40.
2. De Obaldia, M. E., and A. Bhandoola. 2015. Transcriptional regulation of innate and adaptive lymphocyte lineages. *Annu. Rev. Immunol.* 33: 607–642.
3. Kaech, S. M., and W. Cui. 2012. Transcriptional control of effector and memory $CD8^+$ T cell differentiation. *Nat. Rev. Immunol.* 12: 749–761.
4. Iwasaki, A., and R. Medzhitov. 2015. Control of adaptive immunity by the innate immune system. *Nat. Immunol.* 16: 343–353.
5. Roifman, C. M. 2017. Primary T-cell immunodeficiencies. In *Clinical Immunology Principles and Practice*, 5th Ed. R. R. Rich, T. A. Fleisher, W. T. Shearer, H. W. Schroeder, A. J. Frew, and C. M. Weyand, eds. Elsevier, New York, p. 437–453.
6. Altman, A., K. M. Coggeshall, and T. Mustelin. 1990. Molecular events mediating T cell activation. *Adv. Immunol.* 48: 227–360.
7. Linsley, P. S., and J. A. Ledbetter. 1993. The role of the CD28 receptor during T cell responses to antigen. *Annu. Rev. Immunol.* 11: 191–212.
8. Dong, C. 2021. Cytokine regulation and function in T cells. *Annu. Rev. Immunol.* 39: 51–76.
9. Pearce, E. L. 2010. Metabolism in T cell activation and differentiation. *Curr. Opin. Immunol.* 22: 314–320.
10. Gascoigne, N. R., V. Rybakin, O. Acuto, and J. Brzostek. 2016. TCR signal strength and T cell development. *Annu. Rev. Cell Dev. Biol.* 32: 327–348.
11. Carding, S. R., A. C. Hayday, and K. Bottomly. 1991. Cytokines in T-cell development. *Immunol. Today* 12: 239–245.
12. Niu, N., and X. Qin. 2013. New insights into IL-7 signaling pathways during early and late T cell development. *Cell. Mol. Immunol.* 10: 187–189.
13. Zhou, L., M. M. Chong, and D. R. Littman. 2009. Plasticity of $CD4^+$ T cell lineage differentiation. *Immunity* 30: 646–655.
14. Richer, M. J., L. L. Pewe, L. S. Hancox, S. M. Hartwig, S. M. Varga, and J. T. Harty. 2015. Inflammatory IL-15 is required for optimal memory T cell responses. *J. Clin. Invest.* 125: 3477–3490.
15. Peschon, J. J., P. J. Morrissey, K. H. Grabstein, F. J. Ramsdell, E. Maraskovsky, B. C. Gliniak, L. S. Park, S. F. Ziegler, D. E. Williams, C. B. Ware, et al. 1994. Early lymphocyte expansion is severely impaired in interleukin 7 receptor-deficient mice. *J. Exp. Med.* 180: 1955–1960.
16. Kennedy, M. K., M. Glaccum, S. N. Brown, E. A. Butz, J. L. Viney, M. Embers, N. Matsuki, K. Charrier, L. Sedger, C. R. Willis, et al. 2000. Reversible defects in natural killer and memory CD8 T cell lineages in interleukin 15-deficient mice. *J. Exp. Med.* 191: 771–780.
17. Gaffen, S. L., and K. D. Liu. 2004. Overview of interleukin-2 function, production and clinical applications. *Cytokine* 28: 109–123.
18. Liao, W., J. X. Lin, L. Wang, P. Li, and W. J. Leonard. 2011. Modulation of cytokine receptors by IL-2 broadly regulates differentiation into helper T cell lineages. *Nat. Immunol.* 12: 551–559.
19. Liao, W., D. E. Schones, J. Oh, Y. Cui, K. Cui, T. Y. Roh, K. Zhao, and W. J. Leonard. 2008. Priming for T helper type 2 differentiation by interleukin 2-mediated induction of interleukin 4 receptor α-chain expression. *Nat. Immunol.* 9: 1288–1296.

20. Laurence, A., C. M. Tato, T. S. Davidson, Y. Kanno, Z. Chen, Z. Yao, R. B. Blank, F. Meylan, R. Siegel, L. Hennighausen, et al. 2007. Interleukin-2 signaling via STAT5 constrains T helper 17 cell generation. *Immunity* 26: 371–381.
21. Kalia, V., S. Sarkar, S. Subramaniam, W. N. Haining, K. A. Smith, and R. Ahmed. 2010. Prolonged interleukin-2Ralpha expression on virus-specific CD8+ T cells favors terminal-effector differentiation in vivo. *Immunity* 32: 91–103.
22. Pipkin, M. E., J. A. Sacks, F. Cruz-Guilloty, M. G. Lichtenheld, M. J. Bevan, and A. Rao. 2010. Interleukin-2 and inflammation induce distinct transcriptional programs that promote the differentiation of effector cytolytic T cells. *Immunity* 32: 79–90.
23. Boyman, O., and J. Sprent. 2012. The role of interleukin-2 during homeostasis and activation of the immune system. *Nat. Rev. Immunol.* 12: 180–190.
24. Fontenot, J. D., J. P. Rasmussen, M. A. Gavin, and A. Y. Rudensky. 2005. A function for interleukin 2 in Foxp3-expressing regulatory T cells. [Published erratum appears in 2006 *Nat. Immunol.* 7: 427.] *Nat. Immunol.* 6: 1142–1151.
25. Cheng, G., A. Yu, and T. R. Malek. 2011. T-cell tolerance and the multi-functional role of IL-2R signaling in T-regulatory cells. *Immunol. Rev.* 241: 63–76.
26. Willerford, D. M., J. Chen, J. A. Ferry, L. Davidson, A. Ma, and F. W. Alt. 1995. Interleukin-2 receptor α chain regulates the size and content of the peripheral lymphoid compartment. *Immunity* 3: 521–530.
27. Stauber, D. J., E. W. Debler, P. A. Horton, K. A. Smith, and I. A. Wilson. 2006. Crystal structure of the IL-2 signaling complex: paradigm for a heterotrimeric cytokine receptor. *Proc. Natl. Acad. Sci. USA* 103: 2788–2793.
28. Malek, T. R., and I. Castro. 2010. Interleukin-2 receptor signaling: at the interface between tolerance and immunity. *Immunity* 33: 153–165.
29. Cooper, M. D., and M. N. Alder. 2006. The evolution of adaptive immune systems. *Cell* 124: 815–822.
30. Takizawa, F., S. Magadan, D. Parra, Z. Xu, T. Korytář, P. Boudinot, and J. O. Sunyer. 2016. Novel teleost CD4-bearing cell populations provide insights into the evolutionary origins and primordial roles of $CD4^+$ lymphocytes and $CD4^+$ macrophages. *J. Immunol.* 196: 4522–4535.
31. Toda, H., Y. Saito, T. Koike, F. Takizawa, K. Araki, T. Yabu, T. Somamoto, H. Suetake, Y. Suzuki, M. Ototake, et al. 2011. Conservation of characteristics and functions of CD4 positive lymphocytes in a teleost fish. *Dev. Comp. Immunol.* 35: 650–660.
32. Toda, H., Y. Shibasaki, T. Koike, M. Ohtani, F. Takizawa, M. Ototake, T. Moritomo, and T. Nakanishi. 2009. Alloantigen-specific killing is mediated by CD8-positive T cells in fish. *Dev. Comp. Immunol.* 33: 646–652.
33. Wang, T., M. Husain, S. Hong, and J. W. Holland. 2014. Differential expression, modulation and bioactivity of distinct fish IL-12 isoforms: implication towards the evolution of Th1-like immune responses. *Eur. J. Immunol.* 44: 1541–1551.
34. Fischer, U., E. O. Koppang, and T. Nakanishi. 2013. Teleost T and NK cell immunity. *Fish Shellfish Immunol.* 35: 197–206.
35. Zhu, L. Y., P. P. Pan, W. Fang, J. Z. Shao, and L. X. Xiang. 2012. Essential role of IL-4 and IL-4Rα interaction in adaptive immunity of zebrafish: insight into the origin of Th2-like regulatory mechanism in ancient vertebrates. *J. Immunol.* 188: 5571–5584.
36. Zhang, Y.-A., I. Salinas, J. Li, D. Parra, S. Bjork, Z. Xu, S. E. LaPatra, J. Bartholomew, and J. O. Sunyer. 2010. IgT, a primitive immunoglobulin class specialized in mucosal immunity. *Nat. Immunol.* 11: 827–835.
37. Edholm, E. S., E. Bengtén, J. L. Stafford, M. Sahoo, E. B. Taylor, N. W. Miller, and M. Wilson. 2010. Identification of two IgD^+ B cell populations in channel catfish, *Ictalurus punctatus*. *J. Immunol.* 185: 4082–4094.
38. Wei, X., H. Li, Y. Zhang, C. Li, K. Li, K. Ai, and J. Yang. 2020. Ca^{2+}-calcineurin axis-controlled NFAT nuclear translocation is crucial for optimal T cell immunity in an early vertebrate. *J. Immunol.* 204: 569–585.
39. Wei, X., Y. Zhang, C. Li, K. Ai, K. Li, H. Li, and J. Yang. 2020. The evolutionarily conserved MAPK/Erk signaling promotes ancestral T-cell immunity in fish via c-Myc-mediated glycolysis. *J. Biol. Chem.* 295: 3000–3016.
40. Wei, X., C. Li, Y. Zhang, K. Li, J. Li, K. Ai, K. Li, J. Zhang, and J. Yang. 2021. Fish NF-κB couples TCR and IL-17 signals to regulate ancestral T-cell immune response against bacterial infection. *FASEB J.* 35: e21457.
41. Wei, X., K. Ai, H. Li, Y. Zhang, K. Li, and J. Yang. 2019. Ancestral T cells in fish require mTORC1-coupled immune signals and metabolic programming for proper activation and function. *J. Immunol.* 203: 1172–1188.
42. Mu, P., Y. Wang, J. Ao, C. Ai, and X. Chen. 2018. Molecular cloning and bioactivity of an IL-2 homologue in large yellow croaker (*Larimichthys crocea*). *Fish Shellfish Immunol.* 81: 309–317.
43. Ao, J., Y. Mu, L. X. Xiang, D. Fan, M. Feng, S. Zhang, Q. Shi, L. Y. Zhu, T. Li, Y. Ding, et al. 2015. Genome sequencing of the perciform fish *Larimichthys crocea* provides insights into molecular and genetic mechanisms of stress adaptation. *PLoS Genet.* 11: e1005118.
44. Yang, S., Q. Li, Y. Mu, J. Ao, and X. Chen. 2017. Functional activities of interferon gamma in large yellow croaker *Larimichthys crocea*. *Fish Shellfish Immunol.* 70: 545–552.
45. Huang, Y., X. Yuan, P. Mu, Q. Li, J. Ao, and X. Chen. 2019. Development of monoclonal antibody against IgM of large yellow croaker (Larimichthys crocea) and characterization of IgM^+ B cells. *Fish Shellfish Immunol.* 91: 216–222.
46. Ding, Y., C. Ai, Y. Mu, J. Ao, and X. Chen. 2016. Molecular characterization and evolution analysis of five interleukin-17 receptor genes in large yellow croaker *Larimichthys crocea*. *Fish Shellfish Immunol.* 58: 332–339.
47. Livak, K. J., and T. D. Schmittgen. 2001. Analysis of relative gene expression data using real-time quantitative PCR and the $2^{(-\Delta\Delta C(T))}$ method. *Methods* 25: 402–408.
48. Li, C., S. Wang, Q. Ren, T. He, and X. Chen. 2020. An outbreak of visceral white nodules disease caused by *Pseudomonas plecoglossicida* at a water temperature of 12°C in cultured large yellow croaker (*Larimichthys crocea*) in China. *J. Fish Dis.* 43: 1353–1361.
49. Ross, S. H., and D. A. Cantrell. 2018. Signaling and function of interleukin-2 in T lymphocytes. *Annu. Rev. Immunol.* 36: 411–433.
50. Schreiber, S. L., and G. R. Crabtree. 1992. The mechanism of action of cyclosporin A and FK506. *Immunol. Today* 13: 136–142.
51. Mu, P., J. Huo, M. Sun, X. Chen, and J. Ao. 2021. Identification and expression analysis of IL-2 receptors in large yellow croaker (*Larimichthys crocea*). *Fish Shellfish Immunol. Rep.* 2: 100008.
52. Ray, J. P., M. M. Staron, J. A. Shyer, P. C. Ho, H. D. Marshall, S. M. Gray, B. J. Laidlaw, K. Araki, R. Ahmed, S. M. Kaech, and J. Craft. 2015. The interleukin-2-mTORc1 kinase axis defines the signaling, differentiation, and metabolism of T helper 1 and follicular B helper T cells. *Immunity* 43: 690–702.
53. Finlay, D. K., E. Rosenzweig, L. V. Sinclair, C. Feijoo-Carnero, J. L. Hukelmann, J. Rolf, A. A. Panteleyev, K. Okkenhaug, and D. A. Cantrell. 2012. PDK1 regulation of mTOR and hypoxia-inducible factor 1 integrate metabolism and migration of $CD8^+$ T cells. *J. Exp. Med.* 209: 2441–2453.
54. Lin, J.-X., and W. J. Leonard. 2018. The common cytokine receptor γ chain family of cytokines. *Cold Spring Harb. Perspect. Biol.* 10: a028449.
55. Bailey, M., Z. Christoforidou, and M. Lewis. 2013. Evolution of immune systems: specificity and autoreactivity. *Autoimmun. Rev.* 12: 643–647.
56. Liongue, C., R. Sertori, and A. C. Ward. 2016. Evolution of cytokine receptor signaling. *J. Immunol.* 197: 11–18.
57. Malek, T. R. 2008. The biology of interleukin-2. *Annu. Rev. Immunol.* 26: 453–479.
58. D'Souza, W. N., K. S. Schluns, D. Masopust, and L. Lefrançois. 2002. Essential role for IL-2 in the regulation of antiviral extralymphoid CD8 T cell responses. *J. Immunol.* 168: 5566–5572.
59. Cote-Sierra, J., G. Foucras, L. Guo, L. Chiodetti, H. A. Young, J. Hu-Li, J. Zhu, and W. E. Paul. 2004. Interleukin 2 plays a central role in Th2 differentiation. *Proc. Natl. Acad. Sci. USA* 101: 3880–3885.
60. Tang, X., M. Guo, Y. Du, J. Xing, X. Sheng, and W. Zhan. 2019. Interleukin-2 (IL-2) in flounder (*Paralichthys olivaceus*): molecular cloning, characterization and bioactivity analysis. *Fish Shellfish Immunol.* 93: 55–65.
61. Wang, T., Y. Hu, E. Wangkahart, F. Liu, A. Wang, E. Zahran, K. R. Maisey, M. Liu, Q. Xu, M. Imarai, and C. J. Secombes. 2018. Interleukin (IL)-2 is a key regulator of T helper 1 and T helper 2 cytokine expression in fish: functional characterization of two divergent *IL2* paralogs in salmonids. *Front. Immunol.* 9: 1683.
62. Wang, J., W. Wang, J. Xu, Z. Jia, Q. Liu, X. Zhu, C. Xia, and J. Zou. 2021. Structural insights into the co-evolution of IL-2 and its private receptor in fish. *Dev. Comp. Immunol.* 115: 103895.
63. Díaz-Rosales, P., S. Bird, T. H. Wang, K. Fujiki, W. S. Davidson, J. Zou, and C. J. Secombes. 2009. Rainbow trout interleukin-2: cloning, expression and bioactivity analysis. *Fish Shellfish Immunol.* 27: 414–422.
64. Buonocore, F., M. Gerdol, A. Pallavicini, V. Stocchi, E. Randelli, M. C. Belardinelli, A. Miccoli, P. R. Saraceni, C. J. Secombes, G. Scapigliati, and T. Wang. 2020. Identification, molecular characterization and functional analysis of interleukin (IL)-2 and IL-2like (IL-2L) cytokines in sea bass (*Dicentrarchus labrax* L.). *Cytokine* 126: 154898.
65. Olliver, M., J. Hiew, P. Mellroth, B. Henriques-Normark, and P. Bergman. 2011. Human monocytes promote Th1 and Th17 responses to *Streptococcus pneumoniae*. *Infect. Immun.* 79: 4210–4217.
66. Weber, S. E., H. Tian, and L. A. Pirofski. 2011. $CD8^+$ cells enhance resistance to pulmonary serotype 3 *Streptococcus pneumoniae* infection in mice. *J. Immunol.* 186: 432–442.
67. Moriggl, R., D. J. Topham, S. Teglund, V. Sexl, C. McKay, D. Wang, A. Hoffmeyer, J. van Deursen, M. Y. Sangster, K. D. Bunting, et al. 1999. Stat5 is required for IL-2-induced cell cycle progression of peripheral T cells. *Immunity* 10: 249–259.
68. Liu, C., N. M. Chapman, P. W. Karmaus, H. Zeng, and H. Chi. 2015. mTOR and metabolic regulation of conventional and regulatory T cells. *J. Leukoc. Biol.* 97: 837–847.
69. Goldsmith, M. A., S. Y. Lai, W. Xu, M. C. Amaral, E. S. Kuczek, L. J. Parent, G. B. Mills, K. L. Tarr, G. D. Longmore, and W. C. Greene. 1995. Growth signal transduction by the human interleukin-2 receptor requires cytoplasmic tyrosines of the β chain and non-tyrosine residues of the γ c chain. *J. Biol. Chem.* 270: 21729–21737.
70. Wang, T., W. Huang, M. M. Costa, and C. J. Secombes. 2011. The gamma-chain cytokine/receptor system in fish: more ligands and receptors. *Fish Shellfish Immunol.* 31: 673–687.
71. Zhou, X., J. Xing, X. Tang, X. Sheng, and W. Zhan. 2019. Immunological characteristics of Interleukin-2 receptor subunit beta (IL-2Rβ) in flounder (*Paralichtlys olivaceus*): implication for IL-2R function. *Fish Shellfish Immunol.* 93: 641–651.
72. Wang, T., and C. J. Secombes. 2001. Cloning and expression of a putative common cytokine receptor gamma chain (gammaC) gene in rainbow trout (Oncorhynchus mykiss). *Fish Shellfish Immunol.* 11: 233–244.
73. Wang, W., J. Wang, L. Lei, J. Xu, Y. Qin, Q. Gao, and J. Zou. 2020. Characterisation of IL-15 and IL-2Rβ in grass carp: IL-15 upregulates cytokines and transcription factors of type 1 immune response and NK cell activation. *Fish Shellfish Immunol.* 107(Pt A): 104–117.